

# Exact Non-Abelian Supertubes

Ryo Nemoto<sup>1</sup> and Masaki Shigemori<sup>1,2</sup>

<sup>1</sup>Department of Physics, Nagoya University  
Furo-cho, Chikusa-ku, Nagoya 464-8602, Japan

<sup>2</sup>Center for Gravitational Physics,  
Yukawa Institute for Theoretical Physics, Kyoto University  
Kitashirakawa Oiwakecho, Sakyo-ku, Kyoto 606-8502, Japan

Supertubes are supersymmetric configurations in string theory in which branes are extending along a closed curve. For a supertube of codimension two, its dipole charge is characterized by the duality monodromy around the closed curve. When multiple codimension-2 supertubes are present, the monodromies around different supertubes can be non-commuting, namely non-Abelian. Non-Abelian configurations of supertubes are expected to play an important role in non-perturbative physics of string theory, especially black holes. In this paper, in the framework of five-dimensional supergravity, we construct exact solutions describing codimension-2 supertubes in three-dimensional space. We use an extension formula to construct a three-dimensional solution from a two-dimensional seed solution. The two-dimensional seed is an F-theory like configuration in which a torus is nontrivially fibered over a complex plane. In the first example, there is a stack of circular supertubes around which there is a non-trivial monodromy. In some cases this can be thought of as a microstate of a black hole in  $\text{AdS}_2 \times S^2$ . The second example is an axi-symmetric solution with two stacks of circular supertubes with non-Abelian monodromies. In addition, there is a continuous distribution of charges on the symmetry axis.

# Contents

<b>1</b>	<b>Introduction</b>	<b>2</b>
<b>2</b>	<b>Multi-center solutions with codimension 2 and 3</b>	<b>5</b>
2.1	Supersymmetric solutions	5
2.2	Codimension-3 sources	6
2.3	Duality action on harmonic functions	7
2.4	Solutions only with $\tau^3 \equiv \tau$	7
2.5	Codimension-2 solutions	9
<b>3</b>	<b>Extending harmonic functions to 3D</b>	<b>9</b>
3.1	Toroidal coordinate system	10
3.2	2D limit	12
3.3	An extension formula	12
<b>4</b>	<b>Examples</b>	<b>14</b>
4.1	2D solutions from torus fibration	15
4.2	Constant- $\tau$ solutions	16
4.2.1	Constant- $\tau$ solutions in 2D	16
4.2.2	Constant- $\tau$ solutions with a single stack of branes	17
4.3	Non-constant $\tau$ solution with two stacks of branes	21
4.3.1	Charge distributions	26
4.3.2	Absence of closed timelike curves	31
<b>5</b>	<b>Discussions</b>	<b>33</b>
<b>A</b>	<b>Legendre functions and resonant Legendre functions</b>	<b>35</b>
A.1	Legendre functions	35
A.2	Resonant Legendre functions	37
A.3	Relation to harmonic functions	38
<b>B</b>	<b>The ordinary supertube</b>	<b>39</b>
B.1	Partition of unity	41
B.2	The supertube harmonic function expanded in $Q, \bar{Q}$	42
<b>C</b>	<b>More examples</b>	<b>43</b>
C.1	Constant- $\tau$ solutions with two stacks	43
C.2	Another non-constant $\tau$ solution with two stacks	44

# 1 Introduction

Black-hole microstates pose a long-standing puzzle in theoretical physics. Having thermodynamical entropy, black holes must represent ensembles of many microstates, but the gravity picture of those individual microstates remains poorly understood. Some of the black-hole microstates are known to be realized as smooth horizonless solutions of classical supergravity, called microstate geometries. Because supergravity is the low-energy effective theory of string theory, microstate geometries provide a unique, top-down approach to studying the microscopic nature of individual microstates.

The known microstate geometries roughly fall into two categories. The first one is the multi-center solution [1–8], which is a solution of four- or five-dimensional supergravity and represents bound states of branes wrapping internal cycles. The second one is the superstratum [9, 10], which is a solution of six-dimensional supergravity and contains traveling waves along a sixth direction. There are both supersymmetric and non-supersymmetric versions to these solutions, but we restrict ourselves to the supersymmetric solutions which are in better control. The solutions in these two categories both have a large entropy, but it is parametrically smaller than the entropy of the black hole, of which these solutions are microstates [11–13]. Therefore, these solutions correspond to atypical microstates in the relevant black-hole ensembles.

To go beyond these existing microstate geometries and find (more) typical microstates, there are multiple possible directions. One direction is to include full string-theory physics. Typical microstates must certainly be describable in string theory, although it is not completely obvious if full-fledged string theory is necessary for supersymmetric microstates. Another direction is to remain in supergravity but go to higher dimensions by including dependence on more internal directions; see [14–18] for recent work in that direction. Still another direction is to remain in the same supergravity setup of the known microstate geometries but look for more general solutions. In fact, in multi-center solutions, one normally considers brane sources (or centers) that have codimension three, but there are more general solutions with codimension-2 brane sources [19–21]. This extended class of solutions must lead to a larger entropy.

In this paper, we continue the study of multi-center solutions with codimension-2 centers initiated in [19, 20]. Multi-center solutions are supersymmetric solutions of four- or five-dimensional supergravity obtained by compactifying type IIA string theory or M-theory on a Calabi-Yau 3-fold  $X$ . The solution is completely characterized by a set of real harmonic functions on a flat spatial  $\mathbb{R}^3$  base [5]:

$$(V, K^I, L_I, M) \equiv \mathcal{H}, \quad \Delta \mathcal{H} = 0, \quad (1.1)$$

where  $I = 1, \dots, n$  with  $n = h^{1,1}(X)$ , and  $\Delta = \sum_{i=1}^3 (\partial/\partial x_i)^2$ . As harmonic functions,  $\mathcal{H}$

can have codimension-3 (pointlike) sources. Codimension-3 sources in  $V$ ,  $K^I$ ,  $L_I$ , and  $M$  correspond to D6, D4, D2 and D0-branes, respectively, sitting at the location of the source and wrapping cycles in  $X$ . In this paper, we focus on  $X = T^6$  regarded as  $T_{45}^2 \times T_{67}^2 \times T_{89}^2$  (the so-called STU model), and therefore  $I = 1, 2, 3$  ( $n = 3$ ). The harmonic function  $\mathcal{H}$  can also have codimension-2 source along some curve  $\mathcal{C}$  inside  $\mathbb{R}^3$ . A new feature with such codimension-2 sources is that, as we go around  $\mathcal{C}$ , the harmonic functions can undergo a monodromy transformation,

$$\mathcal{H} \rightarrow M\mathcal{H}, \quad (1.2)$$

where  $M$  is an  $(2n + 2) \times (2n + 2)$  matrix representing a  $U$ -duality transformation (for  $X = (T^2)^3$ , the  $U$ -duality group is  $SL(2, \mathbb{Z})^3$ ). In string theory, codimension-2 sources correspond to branes whose worldvolume extends along  $\mathcal{C}$  and, as we go around such a brane, we generally undergo a duality transformation. For example, if we have  $k$  NS5-branes along  $\mathcal{C}$  (with other four spatial directions wrapping internal directions), a component of the NS-NS  $B$ -field jumps by  $k$  units as we go around them. This is a part of  $T$ -duality transformation. Because  $\mathcal{H}$  contains the  $B$ -field, we have a monodromy that can be written as (1.2). Such codimension-2 sources are not mathematical curiosity but very naturally arise in string theory due to the supertube transition [22, 23]. For example, if we have D2(45) and D2(67) branes put together, where 45 and 67 mean wrapped spatial directions, they undergo supertube transition and generically polarize into NS5-branes along 4567 and some other closed curve  $\mathcal{C} \subset \mathbb{R}^3$ .<sup>1</sup> So, we can generally regard codimension-2 sources as *supertubes*, representing the bound states of codimension-3 branes. We will discuss this NS5-brane example in more detail later. As another example, the bound state of D4(6789) and D4(4589) branes is the so-called  $5_2^2$ -brane [24, 25], extending along  $\mathcal{C} \in \mathbb{R}^3$ , and provides a different type of codimension-2 source. Thus, when we study bound states in situations with various branes, taking into account supertube transitions and codimension-2 sources with non-trivial monodromies around them is natural and actually seems unavoidable.

When multiple codimension-2 sources are present, say along  $\mathcal{C}_1$  and  $\mathcal{C}_2$ , it is possible that their monodromy matrices do not commute,  $[M_1, M_2] \neq 0$ . When this happens, we say that the configuration is *non-Abelian*. For example, if NS5 and  $5_2^2$ -branes coexist, their monodromy matrices do not commute and thus the configuration is non-Abelian. In this paper, we will especially be interested in constructing multi-center solutions of non-Abelian supertubes. In [20], some multi-center solutions involving non-Abelian supertubes were constructed in a perturbative approach. However, because of the perturbative nature, certain physical aspects remained unclear, such as the behavior of fields away from the supertubes. In this paper, we will construct examples of exact solutions of non-Abelian supertubes based on the techniques

---

<sup>1</sup>We can also have D4(4567)-brane dipole charge distributed along  $\mathcal{C}$ . There can be other dipole charges but we do not consider them because they will break the symmetry of  $T^6 = T_{45}^2 \times T_{67}^2 \times T_{89}^2$  that we assume.

developed there and clarify their physical aspects, such as charge distributions and absence of closed timelike curves.

When constructing explicit solutions with codimension-2 branes, rather than being general, we focus on the special class of solutions in which the harmonic functions are written in terms of complex harmonic functions  $F, G$  as

$$\begin{aligned} K^1 = K^2 = -\operatorname{Im} G, & \quad L_1 = L_2 = \operatorname{Im} F, \\ L_3 = V = \operatorname{Re} G, & \quad K^3 = -2M = \operatorname{Re} F. \end{aligned} \tag{1.3}$$

Solutions of this restricted class are called SWIP solutions [26]. For this class, the duality group reduces to  $SL(2, \mathbb{Z})$  and the harmonic functions  $(F, G)$  transform as a doublet as we go around codimension-2 branes; namely,

$$\begin{pmatrix} F \\ G \end{pmatrix} \rightarrow M \begin{pmatrix} F \\ G \end{pmatrix}, \quad M = \begin{pmatrix} a & b \\ c & d \end{pmatrix} \in SL(2, \mathbb{Z}), \tag{1.4}$$

where  $a, b, c, d \in \mathbb{Z}$  and  $ad - bc = 1$ . The concrete  $SL(2, \mathbb{Z})$  matrix depends on the specific codimension-2 brane that we consider. So, the problem of constructing solutions with codimension-2 branes amounts to the problem of finding a pair of 3D harmonic functions  $(F, G)$  with the prescribed monodromies. We construct such harmonic functions by starting with a pair of 2D harmonic functions  $(f, g)$  with non-trivial monodromies, and extending them to 3D harmonic functions.

Our first example contains a single stack of  $N$  codimension-2, circular branes around which there is a nontrivial  $SL(2, \mathbb{Z})$  monodromy. Although  $(F, G)$  are nontrivial functions of the coordinates of  $\mathbb{R}^3$ , the ratio  $\tau = F/G$  is constant. If  $N \leq 6$ , this solution is free from closed timelike curves (CTCs) and represent a new microstate of a black hole with a finite horizon with  $\text{AdS}_2 \times S^2$  asymptotics. For  $N = 6$ , the solution takes a particularly simple form:  $F, G \sim [x_1^2 + x_2^2 + (x_3 + iR)^2]^{-1/2}$ . Namely, it is a complexified version of  $1/|\mathbf{x} - \mathbf{a}|$ . The branch cut of the square root leads to the multi-valuedness of the harmonic functions. The second example contains two stacks of codimension-2, circular branes with non-Abelian monodromies.  $\tau$  is not constant but depends on the  $\mathbb{R}^3$  coordinate  $\mathbf{x}$ . This solution was studied in [20] by a perturbative method, but we are presenting the exact version. This solution is free from CTCs but also contains a continuous distribution of codimension-3 charge along the symmetry axis of the configuration, which presumably underpins the stability of the solution. Because this charge density does not decay rapidly enough at infinity, this solution cannot be regarded as a microstate of a black hole.

In Appendix C, we discuss more 3D solutions obtained by extending 2D solutions. Unlike the solutions discussed above, they have a puzzling feature; the 3D solution has a different monodromy structure from the 2D solution that we started with. This is unexpected because extending the solution from 2D to 3D should not change the type of codimension-2 branes

which is characterized by the monodromy. The reason for this phenomenon and the physical relevance of these solutions are unclear and deserve further investigation.

The organization of the paper is as follows. In section 2, we briefly review the multi-center solutions with sources of codimension two and three. In section 3, we discuss how to start with a 2D harmonic function  $h(z)$  defined on a  $z$ -plane with non-trivial monodromies and extend it to a 3D harmonic function  $H(\mathbf{x})$  defined in  $\mathbb{R}^3$ . We present an extension formula that expresses  $H$  in terms of  $h$  by a kind of integral transform. In section 4, we apply the extension formula to some 2D harmonic functions to derive exact 3D harmonic functions with non-trivial monodromies, and discuss their physical properties. Section 5 is devoted to discussion. Appendices contain subjects not covered in the main text. Appendix A explains Legendre functions  $P_\nu, Q_\nu$  as well as resonant Legendre functions  $\mathcal{P}_\nu, \mathcal{Q}_\nu$  that are necessary in constructing harmonic functions with nontrivial monodromies. In Appendix B, we discuss how the ordinary supertube solution fits in the framework of the current paper, where harmonic functions are expanded in the basis of Legendre functions  $P, Q$  and their resonant versions  $\mathcal{P}, \mathcal{Q}$ . In Appendix C, we discuss more exact 3D solutions.

## 2 Multi-center solutions with codimension 2 and 3

In this section we present a lightning review of the multi-center solutions with sources of codimension two and three. The main purpose here is to establish notation. For more detail see [1–8] (for solutions with codimension-2 sources see [19, 20]).

### 2.1 Supersymmetric solutions

Compactification of M-theory on a Calabi-Yau 3-fold  $X$  leads to ungauged 5D  $\mathcal{N} = 1$  supergravity with vector and hypermultiplets. The most general supersymmetric solution of this theory, with hypermultiplets turned off and with a certain condition on  $X$ , were classified in [27] (see also [2, 4, 28]). When we apply this result to  $X = T_{45}^2 \times T_{67}^2 \times T_{89}^2$  and further assume a tri-holomorphic  $U(1)$  symmetry [5], we can reduce the 11D solution to type IIA in ten dimensions, where the general supersymmetric solution takes the following form:

$$\begin{aligned}
 ds_{\text{IIA, str}}^2 &= -\frac{1}{\sqrt{V(Z - V\mu^2)}}(dt + \omega)^2 + \sqrt{V(Z - V\mu^2)}dx_i dx_i \\
 &\quad + \sqrt{\frac{Z - V\mu^2}{V}}(Z_1^{-1}dx_{45}^2 + Z_2^{-1}dx_{67}^2 + Z_3^{-1}dx_{89}^2), \\
 e^{2\Phi} &= \frac{1}{Z} \left( \frac{Z - V\mu^2}{V} \right)^{3/2}, \quad B_2 = \left( \frac{K^I}{V} - \frac{\mu}{Z_I} \right) J_I,
 \end{aligned} \tag{2.1}$$

where  $ds_{\text{IIA, str}}^2$  is the 10D string-frame metric,  $dx_{45}^2 \equiv dx_4^2 + dx_5^2$  etc.,  $J_I \equiv dx_{2I+2} \wedge dx_{2I+3}$ , and  $I = 1, 2, 3$ .  $x_i$  ( $i = 1, 2, 3$ ) are coordinates of a base  $\mathbb{R}^3$ . There are also RR fields turned

on; for their explicit expressions see e.g. [19, App. E] and [29]. Various functions appearing here are defined in terms of the 3D harmonic functions  $\mathcal{H} = (V, K^I, L_I, M)$  (see Eq. (1.1)) as

$$\begin{aligned} Z &= Z_1 Z_2 Z_3, & Z_I &= L_I + \frac{1}{2} C_{IJK} V^{-1} K^J K^K, \\ \mu &= M + \frac{1}{2} V^{-1} K^I L_I + \frac{1}{6} C_{IJK} V^{-2} K^I K^J K^K, \end{aligned} \quad (2.2)$$

where  $C_{IJK} = |\epsilon_{IJK}|$ . The 1-form  $\omega$  is found by solving

$$*d\omega = VdM - MdV + \frac{1}{2}(K^I dL_I - L^I dK_I) = \langle \mathcal{H}, d\mathcal{H} \rangle, \quad (2.3)$$

where  $*$  is the Hodge star for flat  $\mathbb{R}^3$  with metric  $\sum_{i=1}^3 dx_i^2$ . The skew product  $\langle \mathcal{H}, \mathcal{H}' \rangle$  is defined by

$$\langle \mathcal{H}, \mathcal{H}' \rangle \equiv VM' - MV' + \frac{1}{2}(K^I L'_I - L^I K'^I). \quad (2.4)$$

Applying  $d*$  on (2.3) implies the integrability condition [30] (see also [6])

$$0 = \langle \mathcal{H}, \Delta \mathcal{H} \rangle. \quad (2.5)$$

The complexified Kähler modulus for  $T_{89}^2$  is

$$\tau^3 = B_{89} + i\sqrt{\text{vol}(T_{89}^2)} = \left( \frac{K^3}{V} - \frac{\mu}{Z_3} \right) + i \frac{\sqrt{V(Z - V\mu^2)}}{Z_3 V}, \quad (2.6)$$

where the radii of 456789 directions have been all set to  $l_s = \sqrt{\alpha'}$ . The moduli  $\tau^1, \tau^2$  for the tori  $T_{45}^2, T_{67}^2$  are defined similarly. Because the volume of the torus is a real positive number, we must have

$$\text{Im } \tau^I > 0. \quad (2.7)$$

In supergravity,  $\tau^I$  live in the moduli space  $(SL(2, \mathbb{R})/SO(2))^3$ . In string theory, this reduces to  $(SL(2, \mathbb{Z}) \backslash SL(2, \mathbb{R})/SO(2))^3$  due to the  $SL(2, \mathbb{Z})^3$  duality symmetry that identifies different values of  $\tau^I$  as physically equivalent.

## 2.2 Codimension-3 sources

Being harmonic functions,  $\mathcal{H}$  can have codimension-3 (pointlike) sources as

$$\mathcal{H} = h + \sum_{p=1}^N \frac{\Gamma_p}{|\mathbf{x} - \mathbf{a}_p|}. \quad (2.8)$$

The constant  $h = (v_0, k_0^I, l_0^I, m_0)$  determines the value of the moduli at infinity, while  $\Gamma_p = (v_p, k_p^I, l_p^I, m_p)$  represents the D-brane charge at position  $\mathbf{x} = \mathbf{a}_p$  [3]:

$$\begin{aligned} v_p &\leftrightarrow \text{D6}(456789), & k_p^1 &\leftrightarrow \text{D4}(6789), & l_1^p &\leftrightarrow \text{D2}(45) \\ & & k_p^2 &\leftrightarrow \text{D4}(4589), & l_2^p &\leftrightarrow \text{D2}(67), & m_p &\leftrightarrow \text{D0}. \\ & & k_p^3 &\leftrightarrow \text{D4}(4567), & l_3^p &\leftrightarrow \text{D2}(89) \end{aligned} \quad (2.9)$$

The position  $\mathbf{a}_p$  of the sources is not arbitrary but must satisfy the condition

$$\sum_{q(\neq p)} \frac{\langle \Gamma_p, \Gamma_q \rangle}{|\mathbf{a}_p - \mathbf{a}_q|} = \langle h, \Gamma_p \rangle \quad (2.10)$$

that is obtained by requiring that  $\delta$  function terms vanish in the integrability condition (2.5) [6, 30].

### 2.3 Duality action on harmonic functions

The theory with  $X = T_{45}^2 \times T_{67}^2 \times T_{89}^2$  has duality group  $SL(2, \mathbb{Z})_1 \times SL(2, \mathbb{Z})_2 \times SL(2, \mathbb{Z})_3$ , coming from the  $T$ -duality for three individual  $T^2$ s. The eight harmonic functions in  $\mathcal{H}$  transform in the  $(\mathbf{2}, \mathbf{2}, \mathbf{2})$  representation. More concretely, under  $SL(2, \mathbb{Z})_3$  for example, each of the combinations

$$\begin{pmatrix} K^3 \\ V \end{pmatrix}, \quad \begin{pmatrix} 2M \\ -L_3 \end{pmatrix}, \quad \begin{pmatrix} -L_1 \\ K^2 \end{pmatrix}, \quad \begin{pmatrix} -L_2 \\ K^1 \end{pmatrix} \quad (2.11)$$

transforms as a  $\mathbf{2}$ . Namely,

$$\begin{pmatrix} K^3 \\ V \end{pmatrix} \rightarrow M \begin{pmatrix} K^3 \\ V \end{pmatrix} \quad (2.12)$$

where

$$M = \begin{pmatrix} a & b \\ c & d \end{pmatrix}, \quad ad - bc = 1, \quad a, b, c, d \in \mathbb{Z}, \quad (2.13)$$

and likewise for other pairs in (2.11). Under this transformation, the modulus  $\tau^3$  in (2.6) transforms as

$$\tau^3 \rightarrow \frac{a\tau^3 + b}{c\tau^3 + d} \quad (2.14)$$

while  $\tau^{1,2}$  are invariant. We can find transformations under  $SL(2, \mathbb{Z})_{1,2}$  by cyclically permuting the indices in (2.11). In string theory, two configurations related by this duality are different descriptions of the same physics and identified. Therefore, spacetimes patched together by duality transformations are valid backgrounds; for example, we can consider a defect curve  $\mathcal{C}$  around which spacetime is glued by a duality transformation, which is the main topic of the current paper.

### 2.4 Solutions only with $\tau^3 \equiv \tau$

As already discussed in the introduction, we focus on the special class of solutions (called SWIP solutions [26]) in which the eight harmonic functions are determined in terms of two

complex harmonic functions,  $F$  and  $G$ , as in (1.3). In this case, the complexified torus moduli are

$$\tau^1 = \tau^2 = i, \quad \tau^3 = \frac{F}{G} \equiv \tau. \quad (2.15)$$

As mentioned in the introduction (and as can be easily seen using (2.11)), the pair  $(\frac{F}{G})$  transforms as a  $\mathbf{2}$  of  $SL(2, \mathbb{Z})_3$ , and  $\tau$  transforms as

$$\tau \rightarrow \frac{a\tau + b}{c\tau + d}. \quad (2.16)$$

This is a useful subsector in which  $SL(2, \mathbb{Z})_{1,2}$  are switched off. Note that this is not a solution in which branes are wrapping only the third torus  $T_{89}^2$  and the dual 4-cycle. All types of branes in (2.9) are present in a balanced way so that  $T_{45}^2, T_{67}^2$  are kept trivial.

The 10D fields (2.1) become

$$ds_{\text{IIA, str}}^2 = -\frac{1}{|G|^2 \text{Im}(\tau)} (dt + \omega)^2 + |G|^2 \text{Im}(\tau) dx_{123}^2 + dx_{45}^2 + dx_{67}^2 + \text{Im}(\tau) dx_{89}^2, \quad (2.17)$$

$$B_2 = \text{Re}(\tau) dx^8 \wedge dx^9, \quad e^{2\Phi} = \text{Im}(\tau).$$

We clearly see that  $\text{Im}(\tau) > 0$  is necessary for the solution to be physically acceptable. On the other hand, (2.3) becomes

$$*d\omega = \text{Re}(Fd\bar{G} - Gd\bar{F}). \quad (2.18)$$

In the presence of codimension-3 sources, the harmonic functions  $F, G$  can be written as

$$F = h_F + \sum_p \frac{Q_F^p}{|\mathbf{x} - \mathbf{a}_p|}, \quad G = h_G + \sum_p \frac{Q_G^p}{|\mathbf{x} - \mathbf{a}_p|}, \quad (2.19)$$

where the complex quantities  $(h_F, h_G)$  and  $(Q_F^p, Q_G^p)$  are combinations of the real quantities  $h, \Gamma_p$  in (2.8). We will refer to  $(Q_F^p, Q_G^p)$  as complex charges. For generic charges, the centers represent black holes, and the area entropy of the center at  $\mathbf{x} = \mathbf{a}_p$  is

$$S = \frac{\pi |\text{Im}(Q_F^p \bar{Q}_G^p)|}{G_4}, \quad (2.20)$$

where the 4D Newton constant is  $G_4 = g_s^2 l_s^2 / 8$ .

In passing, we mention that a codimension-2 center in the SWIP solutions can describe either a 4-charge 1/8-BPS center or a 2-charge 1/4-BPS center, but not a 3-charge 1/8-BPS center or a 1-charge 1/2-BPS center [20, Appendix D]. A 1-charge 1/2-BPS center is said to be “primitive”, describing a fundamental object in string theory, and played an essential role in constructing microstate geometries with codimension-3 centers [6, 7]. On the other hand, codimension-2 centers in the SWIP solutions can describe a fundamental object in string theory, namely a supertube, which locally preserves 1/2 of supersymmetry [31]. Therefore, the SWIP solution is particularly suited for constructing microstates made of codimension-2 centers.

## 2.5 Codimension-2 solutions

As mentioned in the introduction, we can have codimension-2 solutions, in which the harmonic functions contain codimension-2 sources along a curve  $\mathcal{C} \subset \mathbb{R}^3$  and have a duality monodromy around it as (1.2).

One simple example is the supertube, mentioned in the introduction, for which D2(45) and D2(67) branes polarize into NS5( $\mathcal{C}4567$ )-branes. Let us parametrize the closed curve  $\mathcal{C}$  by  $\mathbf{x} = \mathbf{F}(\lambda)$  with  $0 \leq \lambda \leq 2\pi$ ,  $\mathbf{F}(0) = \mathbf{F}(2\pi)$ . The numbers of D2(45) and D2(67) branes are set to be equal. Then the complex harmonic functions and the modulus  $\tau$  are given by [19]

$$\begin{pmatrix} F \\ G \end{pmatrix} = \begin{pmatrix} h_F + k(\gamma + if) \\ 1 \end{pmatrix}, \quad \tau = h_F + k(\gamma + if), \quad (2.21)$$

where  $k \in \mathbb{Z}$  and the scalars  $f, \gamma$  are defined by

$$f = \frac{1}{4\pi} \int_0^{2\pi} \frac{|\dot{\mathbf{F}}(\lambda)| d\lambda}{|\mathbf{x} - \mathbf{F}(\lambda)|}, \quad \alpha = \frac{dx_i}{4\pi} \int_0^{2\pi} \frac{\dot{F}_i(\lambda) d\lambda}{|\mathbf{x} - \mathbf{F}(\lambda)|}, \quad d\alpha = *d\gamma. \quad (2.22)$$

The harmonicity of  $f, \gamma$  is obvious from the definition. The integrability of the last equation,  $d * d\alpha = 0$ , can be shown using the fact that  $\mathbf{F}(\lambda)$  is periodic. Because  $\gamma$  is nothing but  $\frac{1}{4\pi}$  times the solid angle subtended by  $\mathcal{C}$  measured from  $\mathbf{x}$  [32], it shifts as  $\gamma \rightarrow \gamma + 1$  as we go around  $\mathcal{C}$  (or, of course, this can be more directly shown [19]). Therefore, we have the monodromy

$$\begin{pmatrix} F \\ G \end{pmatrix} \rightarrow M \begin{pmatrix} F \\ G \end{pmatrix}, \quad M = \begin{pmatrix} 1 & k \\ 0 & 1 \end{pmatrix}. \quad (2.23)$$

From (2.17), we see that  $B_2 = (\text{Re}(h_F) + k\gamma) dx_8 \wedge dx_9$ . This shifts by  $k$  units as we go around  $\mathcal{C}$ , which is the correct behavior of  $B_2$  around  $k$  NS5( $\mathcal{C}4567$ )-branes.

It is not so difficult to construct solutions with multiple codimension-2 sources with the same type of monodromy (2.23) with different values of  $k$ , but having multiple codimension-2 sources with non-commuting monodromies is much more challenging, which is the goal of this paper.

In Appendix B, we discuss this standard supertube solution in detail in the framework of the current paper when  $\mathcal{C}$  is a circle.

## 3 Extending harmonic functions to 3D

We would like to study codimension-2 solutions with circular, ring-like sources. In particular, we focus on axisymmetric solutions in which all the rings are parallel to the  $x_1$ - $x_2$  plane and their centers are on the  $x_3$ -axis.

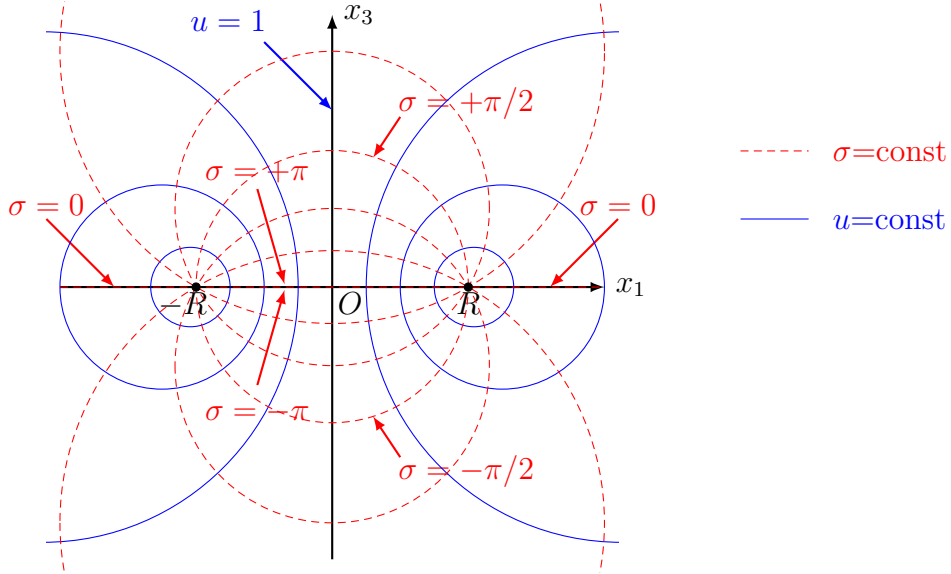


Figure 1: *Toroidal coordinates in the  $x_2 = 0$  section. Blue solid lines represent constant- $u$  surfaces and red dotted lines represent constant- $\sigma$  surfaces. As  $u \rightarrow \infty$  the constant- $u$  surface approaches the circle  $x_1^2 + x_2^2 = R^2, x_3 = 0$ , while as  $u \rightarrow 1$  the the constant- $u$  surface approaches the  $x_3$ -axis if  $\sigma \neq 0$ . If  $\sigma = 0$ , the  $u \rightarrow 1$  limit corresponds to the 3D infinity.*

### 3.1 Toroidal coordinate system

We will initially be interested in situations where the radii of the rings are all approximately  $R$  and their centers are all near the origin, although we will relax this condition later. Let the typical inter-distance between the rings be  $|L| \ll R$ .

In such situations, it is useful to introduce toroidal coordinates  $(u, \sigma, \psi)$ ; see Figure 1. The Cartesian coordinates  $(x_1, x_2, x_3)$  are related to the toroidal coordinates as

$$x_1 + ix_2 = R \frac{\sqrt{u^2 - 1}}{u - \cos \sigma} e^{i\psi}, \quad x_3 = R \frac{\sin \sigma}{u - \cos \sigma}, \quad (3.1)$$

where  $u$  is a “radial” coordinate, and  $\sigma$  and  $\psi$  are the angular variables, respectively, around and along the circle  $\mathcal{C}_0 = \{(x_1, x_2, x_3) \mid x_1^2 + x_2^2 = R^2, x_3 = 0\}$ . The inverse relations are

$$u = \frac{\mathbf{x}^2 + R^2}{\Sigma}, \quad \cos \sigma = \frac{\mathbf{x}^2 - R^2}{\Sigma}, \quad \sin \sigma = \frac{2Rx_3}{\Sigma}, \quad \tan \psi = \frac{x_2}{x_1}, \quad (3.2)$$

with

$$\Sigma = \sqrt{(\mathbf{x}^2 - R^2)^2 + 4R^2x_3^2} = |\mathbf{x}^2 - R^2 \pm 2iRx_3|. \quad (3.3)$$

The flat 3D metric in the toroidal coordinates is given by

$$d\mathbf{x}^2 = \frac{R^2}{(u - \cos \sigma)^2} \left( \frac{du^2}{u^2 - 1} + d\sigma^2 + (u^2 - 1)d\psi^2 \right). \quad (3.4)$$

The range of  $u$  is  $[1, \infty]$ .  $u = \infty$  corresponds to the circle  $\mathcal{C}_0$ , while  $u = 1$  corresponds to the  $\mathbb{R}^3$  infinity (for  $\sigma = 0$ ) and the  $x_3$ -axis (for  $\sigma \neq 0$ ).

The Laplace equation  $\Delta H = 0$  in the toroidal coordinate is separable. If we assume

$$H = \sqrt{u - \cos \sigma} e^{\pm i(\nu + \frac{1}{2})\sigma} h(u), \quad (3.5)$$

we find that  $h$  must satisfy

$$\Delta H \propto [(1 - u^2)\partial_u^2 - 2u\partial_u + \nu(\nu + 1)] h(u) = 0, \quad (3.6)$$

which is the Legendre differential equation. So, the general expression for  $H$  is

$$H(u, \sigma) = \sqrt{u - \cos \sigma} e^{\pm i(\nu + \frac{1}{2})\sigma} (AP_\nu(u) + BQ_\nu(u)) \equiv H_0, \quad (3.7)$$

where  $P_\nu(u)$  and  $Q_\nu(u)$  are the Legendre function of the first and second kinds, respectively.<sup>2</sup>  $P_\nu(u)$  is regular at  $u = 1$  while  $Q_\nu(u)$  goes like  $-\frac{1}{2} \log(u - 1)$  as  $u \rightarrow 1$ . Unless  $\nu \in \mathbb{Z} + 1/2$ , this  $H$  changes by a phase as we go around  $\mathcal{C}_0$  and change  $\sigma \rightarrow \sigma + 2\pi$ .

We can also consider  $H$  that has an additive monodromy. By setting

$$H = \sqrt{u - \cos \sigma} e^{\pm i(\nu + \frac{1}{2})\sigma} (\tilde{h}(u) \pm i\sigma h(u)), \quad (3.8)$$

we find that  $h(u)$  must satisfy (3.6), namely it is given by (3.7), while  $\tilde{h}(u)$  must satisfy the Legendre equation with an inhomogeneous term,

$$[(1 - u^2)\partial_u^2 - 2u\partial_u + \nu(\nu + 1)] \tilde{h}(u) = -(2\nu + 1) h(u). \quad (3.9)$$

This is called the resonant Legendre differential equation [33] and the solution is given by

$$\tilde{h}(u) = AP_\nu(u) + BQ_\nu(u), \quad (3.10)$$

where  $\mathcal{P}_\nu(u) \equiv \partial_\nu P_\nu(u)$ ,  $\mathcal{Q}_\nu(u) \equiv \partial_\nu Q_\nu(u)$  are ‘‘resonant Legendre functions’’ whose detail can be found in Appendix A. The expression for  $H$  is

$$H = \sqrt{u - \cos \sigma} e^{\pm i(\nu + \frac{1}{2})\sigma} \left[ A(\mathcal{P}_\nu(u) \pm i\sigma P_\nu(u)) + B(\mathcal{Q}_\nu(u) \pm i\sigma Q_\nu(u)) \right]. \quad (3.11)$$

As we change  $\sigma \rightarrow \sigma + 2\pi$ , this changes as

$$H \rightarrow e^{\pm 2\pi i(\nu + \frac{1}{2})} (H \pm 2\pi i H_0). \quad (3.12)$$

---

<sup>2</sup>There are different conventions for  $Q_\nu(u)$ , specified by ‘‘type’’. We use  $Q_\nu(u)$  of type 3. See Appendix A for detail.

### 3.2 2D limit

Let us consider zooming in onto the region near  $\mathbf{x} = (R, 0, 0)$ . In this limit, rings near that point look like straight lines along  $x_2$ . This limit can be taken by sending  $u \rightarrow +\infty$ ,  $\psi \rightarrow 0$ , for which

$$x_1 \approx R + \frac{R}{u} \cos \sigma, \quad x_2 \approx 0, \quad x_3 \approx \frac{R}{u} \sin \sigma. \quad (3.13)$$

If we regard the  $x_1$ - $x_3$  plane as a complex  $z$ -plane, identifying  $(x_1, x_3) = (R, 0)$  with the origin  $z = 0$ , then we have the following relation:

$$z \approx (x_1 - R) + ix_3 \approx \frac{R}{u} e^{i\sigma}. \quad (3.14)$$

In this limit, the metric becomes that of flat  $z$ -plane (ignoring  $x_2$ ) and the Laplace equation reduces to  $\partial_z \partial_{\bar{z}} H = 0$ , meaning that  $H$  is a sum of holomorphic and anti-holomorphic functions. We will refer to this limit as the *2D limit*.

### 3.3 An extension formula

In the 2D limit, the 3D Laplace equation reduces to the 2D Laplace equation, whose solution is  $H_{2D}(z) = h(z) + \tilde{h}(\bar{z})$ . Given such  $H_{2D}(z)$ , is it possible to extend it to a solution of the 3D Laplace equation that is defined in the entire  $\mathbb{R}^3$ ? The answer to this problem can be found by a matching technique discussed in [20], although a closed expression was not presented there.

Assume that we have a 2D solution  $H_{2D} = h(z)$ , which we assume to be holomorphic (generalization to include an anti-holomorphic part is straightforward). If the 2D solution has no source at  $z = \infty$ , then  $h(z)$  must be expandable in  $1/z$  as

$$h(z) = \sum_k \frac{a_k}{\hat{z}^{k+\frac{1}{2}}}, \quad \hat{z} \equiv \frac{z}{L}, \quad (3.15)$$

where  $k + 1/2 > 0$  but  $k$  is not necessarily an integer. The constant  $L$  determines the scale of the 2D solution and can be complex in general:

$$L = |L| e^{il}, \quad l \in \mathbb{R}. \quad (3.16)$$

We can scale the size of the structure of the 2D solution by changing  $L$ . Then the expression for  $H(u, \sigma)$  that extends  $h(z)$  to the entire  $\mathbb{R}^3$  is

$$H(u, \sigma) = \sqrt{\frac{u - \cos \sigma}{Z}} \sum_k \frac{2^k (k!)^2 a_k}{(2k)! Z^k} P_k(u) \quad (3.17a)$$

$$= \sqrt{\frac{u - \cos \sigma}{Z}} \sum_k \frac{(k!)^2 a_k}{(2k)!} \frac{1}{2\pi i} \oint_C \frac{dt}{t - u} \left[ \frac{t^2 - 1}{(t - u)Z} \right]^k, \quad (3.17b)$$

where

$$Z \equiv \frac{R}{L} e^{i\sigma} \quad (3.18)$$

and in the second equality we used the Schläfli integral representation of the Legendre function, (A.2). We will denote a 2D solution by a lowercase letter and the corresponding 3D solution by a capital letter. We will henceforth refer to (3.17) as the extension formula.

We can readily check that the 3D harmonic function (3.17a) reduces to the 2D expression (3.15) in the following sense. We can go to the  $z$ -plane by considering  $u \rightarrow \infty$ , with the dictionary (3.14)

$$z \leftrightarrow \frac{R}{u} e^{i\sigma} = \frac{LZ}{u}, \quad \text{or} \quad \hat{z} \leftrightarrow \frac{Z}{u}. \quad (3.19)$$

Furthermore, let us simultaneously send  $\frac{L}{R} \rightarrow 0$  so that the inter-distance between rings is much smaller than their radii. Concretely, we send

$$Z, u \rightarrow \infty \quad \text{with} \quad \hat{z} = \frac{Z}{u} \text{ fixed.} \quad (3.20)$$

Namely, we zoom in onto the region near  $\mathbf{x} = (R, 0, 0)$  and, at the same rate, scale down the ring structure, so that we end up with a non-trivial structure on the  $z$ -plane. If we take this limit and use the relation (see (A.11))

$$P_k(u) \rightarrow \frac{(2k)!}{2^k (k!)^2} u^k \quad (u \rightarrow \infty), \quad (3.21)$$

it is easy to see that (3.17a) reduces to (3.15). We will refer to the limit (3.20) as the *scaling limit*.

We have not specified the integration contour  $C$  in (3.17b). In the Schläfli integral (A.2), the contour for  $P_k(u)$  goes counterclockwise around the pole  $t = u$  if  $k \in \mathbb{Z}$  and around the logarithmic branch cut  $[1, u]$  if  $k \notin \mathbb{Z}$ . Because of the infinite sum, the integrand of the  $t$  integral (3.17b) may develop extra branch cuts. In that case, we may have to enlarge  $C$  to enclose them. The correct choice for  $C$  is determined by the requirement that it reproduce the 2D harmonic function  $h(z)$  in the scaling limit.

The above  $H$  is not a unique 3D harmonic function that reduces to the given 2D one in the scaling limit. We can add to  $a_k$  a number, such as  $(L/R)^n$  with  $n > 0$ , which vanishes in the scaling limit. Also, we could have included  $Q_k(u)$  in (3.17a), because it vanishes as  $u \rightarrow \infty$  for  $k > -1$  and would not change the scaling limit of  $H$ . However, including  $Q_k(u)$  leads to divergent  $H$  in 3D, because  $Q_k(u)$  blows up logarithmically at  $u = 1$ .

Another expression for  $H(u, \sigma)$  is

$$H(u, \sigma) = \sqrt{\frac{u - \cos \sigma}{Z}} \frac{1}{2\pi i} \oint_C \frac{dt}{t - u} \int_0^1 dy h' \left( \frac{Z(t - u)}{y(1 - y)(t^2 - 1)} \right) \quad (3.22)$$

where

$$h'(\hat{z}) \equiv \sum_k (2k+1)a_k \hat{z}^{-k} = -2\hat{z}^{3/2} \frac{dh}{d\hat{z}}. \quad (3.23)$$

The above expression can be derived using the identity

$$\frac{(k!)^2}{(2k)!} = (2k+1) \int_0^1 dy y^k (1-y)^k. \quad (3.24)$$

Being a sum of harmonic functions, the function  $H$  as given in (3.17a) must be harmonic. We can make the harmonicity of  $H$  manifest by going to  $w$  defined by

$$w = \frac{t^2 - 1}{a(t-u)Z}, \quad (3.25)$$

where  $a$  is constant, so that

$$t = \frac{aZ}{2} \left( w + \sqrt{w^2 - \frac{4u}{aZ}w + \frac{4}{a^2Z^2}} \right), \quad \frac{dt}{t-u} = \frac{dw}{\sqrt{w^2 - \frac{4u}{aZ}w + \frac{4}{a^2Z^2}}}. \quad (3.26)$$

The expression (3.17b) now takes the form

$$\sqrt{\frac{u - \cos \sigma}{Z}} \oint \frac{dt}{t-u} \Phi \left( \frac{t^2 - 1}{a(t-u)Z} \right) = \sqrt{\frac{u - \cos \sigma}{Z}} \oint \frac{\Phi(w) dw}{\sqrt{w^2 - \frac{4u}{aZ}w + \frac{4}{a^2Z^2}}} \quad (3.27)$$

with a suitable function  $\Phi$ . One can easily check that the integrand in the last expression is harmonic for any  $w$ . Therefore, this is harmonic for an arbitrary function  $\Phi(w)$ , as long as the specification of the contour  $C$  does not depend on  $u, \sigma$ . This arbitrariness corresponds to the arbitrary holomorphic function in the 2D limit. Anti-holomorphic functions correspond to setting  $Z \rightarrow \bar{Z}$  in this expression. The contour  $C$  in the  $t$ -plane can often be deformed in the  $w$  coordinate into a contour encircling the branch cut  $[w_-, w_+]$ , where  $w_{\pm}$  are the roots of the radicand in (3.27):

$$w^2 - \frac{4u}{aZ}w + \frac{4}{a^2Z^2} = (w - w_+)(w - w_-), \quad w_{\pm} = \frac{2}{aZ}(u \pm \sqrt{u^2 - 1}). \quad (3.28)$$

For large positive  $Z$  ( $\gg u$ ), we have  $0 < w_- < w_+ < 1$ .

## 4 Examples

Let us take some simple examples of 2D solutions  $(f(z), g(z))$ , apply the extension formula (3.17) to them to construct 3D solutions  $(F(u, \sigma), G(u, \sigma))$ , and discuss their properties.

## 4.1 2D solutions from torus fibration

We would like to start with some 2D harmonic functions  $(f(z), g(z))$  as a seed. They are holomorphic functions which undergo nontrivial  $SL(2, \mathbb{Z})$  monodromies as we go around branes which are pointlike on the  $z$ -plane. Moreover, their ratio  $f/g = \tau$  must satisfy  $\text{Im } \tau > 0$ . The standard way to construct such  $(f, g)$ , used e.g. in the Seiberg-Witten theory [34, 35] and F-theory [36, 37], is to consider fibration of a torus over the  $z$ -plane and regard  $(f, g)$  as the periods of the torus.

Concretely, consider a torus in the Weierstrass form:

$$y^2 = x^3 + p(z)x + q(z). \quad (4.1)$$

where  $p(z), q(z)$  are polynomials in  $z$ . The modulus  $\tau$  of the torus is known to be given by

$$j(\tau) = \frac{4(24p)^3}{4p^3 + 27q^2}. \quad (4.2)$$

where  $j(\tau)$  is Klein's  $j$ -invariant<sup>3</sup> with a  $q$ -expansion

$$j(\tau) = 2^3(q^{-1} + 744 + 196884q + \dots), \quad q = e^{2\pi i \tau}. \quad (4.3)$$

If we want to control the value of  $\tau$  at  $z = \infty$ , the degree of  $p(z)$  and  $q(z)$  must be  $N/3$  and  $N/2$  with some  $N$ . For the degree of  $p(z), q(z)$  to be integral,  $N$  must be an integer multiple of 6.

The periods of the torus (4.1) are given by the integral of the unique holomorphic 1-form  $\lambda = dx/y$  along the  $A$  and  $B$  cycles:

$$f(z) = \oint_A \frac{dx}{\sqrt{x^3 + p(z)x + q(z)}}, \quad g(z) = \oint_B \frac{dx}{\sqrt{x^3 + p(z)x + q(z)}}. \quad (4.4)$$

For large  $|z|$ , by setting  $x \rightarrow z^{\frac{N}{6}}x$ , we can show that these generically go like  $z^{-\frac{N}{12}}$ . These periods give a different expression for the modulus,

$$\tau(z) = \frac{f(z)}{g(z)}. \quad (4.5)$$

The discriminant of the cubic polynomial on the right hand side of (4.1),

$$\Delta = 4p^3 + 27q^2, \quad (4.6)$$

vanishes when some branch points collide and the torus becomes singular. Indeed, from (4.2) and (4.3), we see that  $\text{Im } \tau \rightarrow \infty$  at these points (unless  $p = 0$  there). They give the values of  $z$  at which branes are located. Because  $\Delta$  has degree  $N$ , there are  $N$  branes generically. As we move in the  $z$  space around these branes, the cycles  $A, B$  undergo non-trivial  $SL(2, \mathbb{Z})$  monodromies and so do the associated harmonic functions  $f, g$ .

---

<sup>3</sup>Our convention is such that  $j(i) = 24^3$ ,  $j(e^{2\pi i/3}) = 0$ .

## 4.2 Constant- $\tau$ solutions

### 4.2.1 Constant- $\tau$ solutions in 2D

Given the functions  $p(z)$  and  $q(z)$ , equation (4.1) describes fibration of a torus on the  $z$ -plane. One particularly simple case is when  $\tau(z)$  is constant independent of  $z$  (but the harmonic functions  $f(z), g(z)$  are generally nontrivial). There are three cases in which  $\tau(z)$  is constant [38, 39]:

(i)  $p(z) = 0$ :

In this case, we have  $N \in 2\mathbb{Z}$  and

$$j(\tau) = 0, \quad \tau = e^{2\pi i/3}, \quad q \propto \prod_{i=1}^{N/2} (z - z_i), \quad \Delta \propto \prod_{i=1}^{N/2} (z - z_i)^2. \quad (4.7)$$

The 2D harmonic functions (4.4) are

$$g = c \prod_i^{N/2} (z - z_i)^{-1/6}, \quad f = e^{2\pi i/3} g, \quad (4.8)$$

where  $c$  is constant. There are 2 branes at each  $z_i$ . Around each stack of branes, there are an  $SL(2, \mathbb{Z})$  monodromy  $\begin{pmatrix} -1 & 1 \\ -1 & 0 \end{pmatrix}$ , which has order 6, and a deficit angle  $\pi/3$ .

(ii)  $q(z) = 0$ :

In this case, we have  $N \in 3\mathbb{Z}$  and

$$j(\tau) = 24^3, \quad \tau = i, \quad p \propto \prod_{i=1}^{N/3} (z - z_i), \quad \Delta \propto \prod_{i=1}^{N/3} (z - z_i)^3. \quad (4.9)$$

The 2D harmonic functions are

$$g = c \prod_i^{N/3} (z - z_i)^{-1/4}, \quad f = i g, \quad (4.10)$$

where  $c$  is constant. There are 3 branes at each  $z_i$ . Around each stack of branes, there are an  $SL(2, \mathbb{Z})$  monodromy  $\begin{pmatrix} 0 & 1 \\ -1 & 0 \end{pmatrix}$ , which has order 4, and a deficit angle  $\pi/2$ .

(iii)  $p(z)^3 = \alpha^3 q(z)^2$ ,  $\alpha = \text{const}$ :

In this case, we have  $N \in 6\mathbb{Z}$  and

$$j(\tau_0) = \frac{4 \cdot 24^3 \alpha^3}{4\alpha^3 + 27}, \quad q \propto \prod_{i=1}^{N/6} (z - z_i)^3, \quad p \propto \alpha \prod_{i=1}^{N/6} (z - z_i)^2, \quad \Delta \propto \prod_{i=1}^{N/6} (z - z_i)^6. \quad (4.11)$$

The 2D harmonic functions are

$$g = c \prod_i^{N/6} (z - z_i)^{-1/2}, \quad f = \tau_0 g, \quad (4.12)$$

where  $c$  is constant while  $\tau_0$  is the constant determined by the first equation in (4.11). There are 6 branes at each  $z_i$ . Around each stack of branes, there are an  $SL(2, \mathbb{Z})$  monodromy  $\begin{pmatrix} -1 & 0 \\ 0 & -1 \end{pmatrix}$ , which has order 2, and a deficit angle  $\pi$ .

### 4.2.2 Constant- $\tau$ solutions with a single stack of branes

Here we apply the extension formula (3.17) to the case where there is a single stack of  $N$  branes sitting at  $z = 0$ . We take  $N$  to be general, not specifying which of the cases (i)–(iii) we are considering. The 2D harmonic functions are

$$g = z^{-N/12}, \quad f = \tau_0 z^{-N/12}, \quad (4.13)$$

where  $\tau_0$  is the constant value of the torus modulus which depends on the cases (i)–(iii).  $N$  can be an integer multiple of 2, 3, or 6, depending on the case (i), (ii) or (iii). There can be an overall constant which we ignore at this point.

There being only one term in the  $1/z$  expansion, the 3D harmonic function can immediately be found using (3.17):

$$\begin{aligned} G &= \frac{c}{R} \sqrt{u - \cos \sigma} e^{-i \frac{N}{12} \sigma} P_{\frac{N}{12} - \frac{1}{2}}(u) \\ &= \frac{c}{\sqrt{\Sigma}} \left( \frac{\mathbf{x}^2 - R^2 - 2iRx_3}{\Sigma} \right)^{\frac{N}{12}} P_{\frac{N}{12} - \frac{1}{2}}(u), \end{aligned} \quad (4.14)$$

and

$$F = \tau_0 G. \quad (4.15)$$

In the above,

$$c = \frac{2^{\frac{N}{12}} \Gamma(\frac{N}{12} + \frac{1}{2})^2}{\Gamma(\frac{N}{6})} \left( \frac{L}{R} \right)^{\frac{N}{12}} R, \quad (4.16)$$

but we can replace this  $c$  by an arbitrary complex number, absorbing the arbitrary overall complex number that we could have multiplied  $f, g$  by.

The large  $r = |\mathbf{x}|$  behavior is

$$G = \frac{Q_G}{r} + \dots, \quad F = \frac{Q_F}{r} + \dots, \quad (4.17)$$

where

$$Q_G = c, \quad Q_F = c\tau_0. \quad (4.18)$$

Therefore, seen from far away, the ring looks like a codimension-3 center with complex charges  $(Q_G, Q_F)$  and a black-hole entropy (2.20) which becomes

$$S = \frac{\pi |c|^2 \text{Im}(\tau_0)}{G_4}. \quad (4.19)$$

So, this configuration can be regarded as a microstate of a black hole. Note that there is no constant term in (4.17) and hence this configuration is asymptotically  $\text{AdS}_2 \times S^2$ . This is due

to the non-trivial monodromy around the ring; a constant in the harmonic function would be inconsistent with the monodromy. Although this solution must be locally 1/2-BPS, it is not a smooth geometry and is therefore a microstate solution rather than a microstate geometry according to the terminology of [40].

Let us study the properties of the solution. From (2.18), we find

$$*d\omega = -\frac{|c|^2 N (\text{Im } \tau_0)}{6R^2} (u - \cos \sigma) P_{\frac{N}{12} - \frac{1}{2}}(u)^2 d\sigma. \quad (4.20)$$

Integrating this equation, we obtain

$$\omega = \frac{|c|^2 N \text{Im}(\tau_0)}{6R} \left( \int_1^u P_{\frac{N}{12} - \frac{1}{2}}(u)^2 du \right) d\psi, \quad (4.21)$$

where we chose the constant of integration so that this vanishes at the 3D infinity ( $u = 1$ ). Using the  $u \rightarrow 1$  behavior of  $P_\nu(u)$ , we find that the large  $r$  behavior of  $\omega$  is

$$\omega = \frac{|c|^2 N R \text{Im}(\tau_0) \sin^2 \theta}{3r^2} d\psi + \dots. \quad (4.22)$$

Because angular momentum  $J$  is read off from the  $\mathcal{O}(1/r)$  term in  $\omega$ , we see that  $J = 0$ . This is as it should be, because of the  $\text{AdS}_2$  asymptotics. This is interesting in view of the claim [41–43] that genuine black-hole microstates must have  $J = 0$ .

By looking at the metric (2.17), we see that the  $\psi$  direction potentially develops CTCs. Using the above expression for  $\psi$ , we find that the  $\psi\psi$  component of the metric is

$$g_{\psi\psi} = \frac{(\text{Im } \tau)|c|^2}{(u - \cos \sigma) P_{\frac{N}{12} - \frac{1}{2}}(u)^2} \left[ -\left(\frac{N}{6}\right)^2 \left( \int_1^u P_{\frac{N}{12} - \frac{1}{2}}(u)^2 \right)^2 + (u^2 - 1) P_{\frac{N}{12} - \frac{1}{2}}(u)^4 \right]. \quad (4.23)$$

Using the large  $u$  behavior of  $P_{\frac{N}{12} - \frac{1}{2}}(u)$ , we can show that  $g_{\psi\psi}$  is non-negative everywhere for  $N \leq 6$ . However, if  $N > 6$ , the  $g_{\psi\psi}$  becomes negative near the ring and the  $\psi$  direction becomes a CTC. So, only  $N \leq 6$  solutions are physically acceptable. This is unlike F-theory 7-branes, along which metric is regular. This is because our branes are not made of a single species of branes but are supertubes with lower charges dissolved in the worldvolume.

Next, let us look at the geometry in the directions orthogonal to  $\psi$ , namely  $(u, \sigma)$  directions. Near the ring,  $u = \infty$ , we find that the  $u, \sigma$  part of the metric goes like

$$\begin{aligned} ds^2 &\sim \tau_2 |c|^2 R^2 \left( \frac{|L|}{R} \right)^{N/6} u^{\frac{N}{6} - 2} \left( \frac{du^2}{u^2} + d\sigma^2 \right) \\ &\sim |c|^2 R^2 \left( \frac{|L|}{R} \right)^{N/6} \rho^{-\frac{N}{6}} (d\rho^2 + \rho^2 d\sigma^2) \end{aligned} \quad (4.24)$$

where  $\rho \equiv 1/u$ . This is a conical deficit geometry with opening angle  $2\pi(1 - \frac{N}{12})$ . The distance to the position of the brane,  $\rho = 0$  ( $u = \infty$ ), is

$$\sim \int_\epsilon \rho^{-N/12} d\rho = \left[ \frac{\rho^{1-N/12}}{1 - N/12} \right]_\epsilon \quad (4.25)$$

where  $\epsilon \ll 1$  is a cutoff. This is finite for  $N < 12$  but, for  $N > 12$ , the distance diverges. If  $N = 12$ , the distance is logarithmically divergent. Recall that, in F-theory, 7-branes introduce conical deficits in the 2-dimensional base space; if  $N \leq 12$ , the base is noncompact but, if  $N \geq 12$ , the base space becomes compact (for  $N = 12$  the base becomes a half-infinite capped cylinder, while for  $N = 24$  it becomes  $S^2$ ). This is showing up in our context as the branes becoming unreachable from asymptotic infinity in the  $N \geq 12$  case.

•  **$N = 6$**

Let us discuss in some detail the  $N = 6$  case, where expressions are simple and where there are no physical subtleties discussed above. The 3D harmonic function (4.14) is simply

$$G = \frac{c}{R} \sqrt{u - \cos \sigma} e^{-i\sigma/2} = \frac{c}{\sqrt{x_1^2 + x_2^2 + (x_3 + iR)^2}}. \quad (4.26)$$

We see the branch “point” at  $x_1^2 + x_2^2 = R^2$ ,  $x_3 = 0$  explicitly; we get a minus sign as we go through the ring. Flipping the sign of all harmonic functions at once does not lead to issues like a wrong signature of the metric, because the signs cancel in the combinations that enter the metric. Near this branch point,  $G$  goes like  $u^{1/2} \sim 1/\sqrt{z}$ , as expected from  $g = 1/\sqrt{z}$ . That this is harmonic is clear because this is  $[(\mathbf{x} - \mathbf{a})^2]^{-1/2}$  with  $\mathbf{a} = (0, 0, -iR)$ . This type of harmonic function appeared in [1] in a different context.

One may wonder if we can put this brane at multiple places, so that

$$G \stackrel{?}{=} \frac{c}{\sqrt{x_1^2 + x_2^2 + (x_3 + iR)^2}} + \frac{c'}{\sqrt{x_1^2 + x_2^2 + (x_3 + iR')^2}}, \quad (4.27)$$

which is certainly harmonic. However, this is not physically allowed because this screws up the monodromy. Going around once around the branes will flip the sign of only one term, whereas the  $SL(2, \mathbb{Z})$  transformation (which is  $\begin{pmatrix} -1 & 0 \\ 0 & -1 \end{pmatrix}$  in this case) must act on the entire  $G$ .

The 1-form  $\omega$  is given by

$$\omega = \frac{|c|^2 \text{Im}(\tau_0)}{R} (u - 1) d\psi = \frac{|c|^2 \text{Im}(\tau_0)}{R} \left( \frac{r^2 + R^2}{\Sigma} - 1 \right) d\psi, \quad (4.28)$$

which is well-behaved and vanishes at infinity. One can show that the Komar form,  $\epsilon_{\alpha\beta\mu\nu} \nabla^\alpha \xi^\beta$  where  $\xi = \partial_\psi$ , has vanishing spatial components. Therefore, these branes carry no angular momentum even locally; this is quite different from ordinary supertubes, which carry angular momentum by worldvolume fluxes.

The  $\psi\psi$  component of the metric, (4.23), is

$$g_{\psi\psi} = 2(\text{Im } \tau) |c|^2 \frac{u - 1}{u - \cos \sigma} \quad (4.29)$$

which is positive everywhere. The  $\psi$  circle is finite even on the ring ( $u \rightarrow \infty$ ) which is unlike ordinary supertubes along which the metric gets null [23]. This is because the current solution

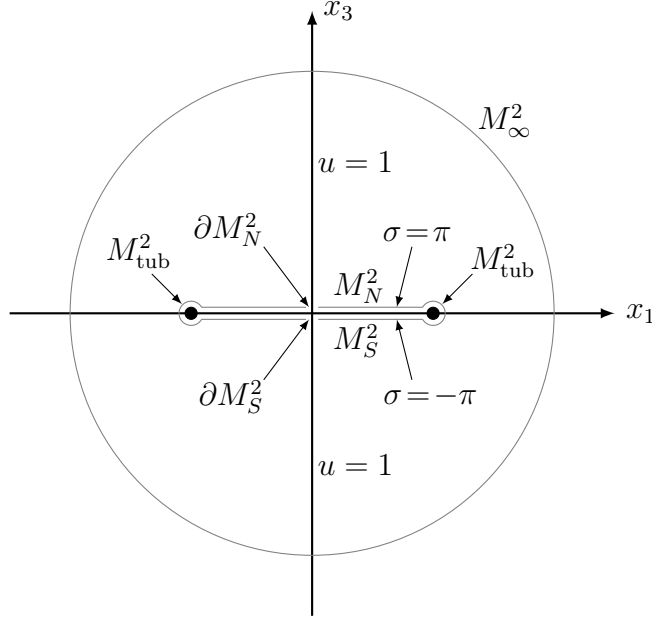


Figure 2: Gaussian surface..

is not an ordinary supertube but a limit in which multiple supertubes with non-commuting monodromies collapse to a point [38, 39].

We know that the total charge is given by (4.18), but let us study its distribution in some detail. The charge can be measured by

$$Q_G = -\frac{1}{4\pi} \int_{M^2} *dG \quad (4.30)$$

where  $M^2$  is a Gaussian surface enclosing the entire branes. We can take it to be  $M_\infty^2$  in Figure 2. If  $G$  were single-valued, we could freely deform it as long as singular sources are avoided. However, in the present case where  $G$  is multi-valued, we cannot deform  $M^2$  into a tubular surface enclosing just the branes. As in Figure 2, we can deform  $M_\infty^2$  into a tubular surface  $M_{\text{tub}}^2$  plus two disks,  $M_N^2$  and  $M_S^2$ , that are at  $\sigma = \pi$  and  $\sigma = -\pi$ , respectively, and touch the branes from inside. In the present case,

$$*dG = ce^{-i\sigma/2} \frac{i(u - e^{-i\sigma})du + (u^2 - 1)d\sigma}{\sqrt{2}(u - \cos \sigma)^{3/2}} \wedge d\psi. \quad (4.31)$$

The contribution from  $M_{\text{tub}}^2$  is

$$-\frac{1}{4\pi} \int_{M_{\text{tub}}^2} *dG = \frac{1}{2} \int_{-\pi}^{\pi} \frac{ce^{-i\sigma/2}(u^2 - 1)}{2(u - \cos \sigma)^{3/2}} d\sigma \Big|_{u=u_c} = c\sqrt{2u_c}, \quad (4.32)$$

where  $u_c \gg 1$  is a regulator. The contribution from  $M_N^2$  and  $M_S^2$  is

$$-\frac{1}{4\pi} \int_{M_N^2 + M_S^2} *dG = \frac{1}{2} \int_1^{u_c} \left[ ce^{-i\sigma/2} \frac{i(u - e^{-i\sigma})}{2(u - \cos \sigma)^{3/2}} du \right]_{\sigma=-\pi}^{\sigma=\pi} = c(1 - \sqrt{2u_c}). \quad (4.33)$$

So, the Gaussian integration over the tubular region  $M_{\text{tub}}^2$  and the disks  $M_{N,S}^2$  individually diverge, but their sum is finite and equal to (4.18). The same holds for  $Q_F$ . The disk  $M_{N,S}^2$  carrying charge by the multi-valuedness of fluxes is an example of the so-called Cheshire charge that appears in the presence of vortices with non-trivial monodromies called Alice strings [44–46] (for Alice strings in string theory, see [47, 48]).

Alternatively, we can compute the same Gaussian integral using the 1-form  $\mathcal{G}$  that satisfies

$$*dG = d\mathcal{G}, \quad (4.34)$$

with which (4.30) can be written as

$$Q_G = -\frac{1}{4\pi} \int_{\partial M^2} \mathcal{G}. \quad (4.35)$$

This way of computing the charge will be useful in the example discussed later. In the present case,  $\mathcal{G}$  is given by

$$\mathcal{G} = \frac{ic(u - e^{i\sigma})e^{-i\sigma/2}}{\sqrt{u - \cos \sigma}} d\psi. \quad (4.36)$$

This  $\mathcal{G}$  has Dirac strings on the  $x_3$ -axis. So, as the boundary of the Gaussian surface  $M^2 = M_{\text{tub}}^2 \cup M_N^2 \cup M_S^2$ , we can take small circles around the  $x_3$ -axis at  $\sigma = \pi$  ( $\partial M_N^2$ ) and at  $\sigma = -\pi$  ( $\partial M_S^2$ ). At  $u = 1$ ,

$$\mathcal{G}|_{u=1} = c \operatorname{sign}(\sin \frac{\sigma}{2}) d\psi. \quad (4.37)$$

Therefore, by adding the contributions from the north and south poles, we obtain

$$Q_G = -\frac{1}{4\pi}(-2\pi c - 2\pi c) = c, \quad (4.38)$$

which is the same as (4.18).

We can do a similar analysis for other values of  $N$ .

### 4.3 Non-constant $\tau$ solution with two stacks of branes

As a more nontrivial example, consider the following torus:

$$y^2 = (x^2 - 1)(x - \hat{z}). \quad (4.39)$$

By shifting  $x$ , we can bring this curve into the Weierstrass form (4.1), with

$$p = -\left(\frac{\hat{z}^2}{3} + 1\right), \quad q = -\frac{2}{27}\hat{z}(\hat{z}^2 - 9), \quad (4.40)$$

which corresponds to  $N = 6$ . Eq. (4.2) becomes

$$j(\tau) = \frac{f(z)}{g(z)} = \frac{512(\hat{z}^2 + 3)^3}{(\hat{z}^2 - 1)^2}. \quad (4.41)$$

By looking at the values of  $\hat{z}$  at which the right-hand side diverges and the order of the divergence, we see that there are two branes at  $\hat{z} = 1$  and another two branes at  $\hat{z} = -1$ . These are points where the discriminant  $\Delta$  vanishes. In addition, the right-hand side diverges at  $\hat{z} = \infty$ , implying that there are two branes at  $\hat{z} = \infty$ . In terms of  $z = L\hat{z}$ , the branes are at  $z = \pm L, \infty$ .

In [20], the 3D extension of the 2D harmonic functions based on the the curve (4.39) was studied by a perturbative approach. Here we use the extension formula (3.17) to study the exact 3D extension. The curve (4.39) is the Seiberg-Witten curve for pure  $\mathcal{N} = 2$   $SU(2)$  Yang-Mills theory [34], describing the vacuum moduli space parametrized by the vev of the adjoint scalar. Here we are borrowing the curve as a simple example of torus fibration that gives non-trivial 2D harmonic functions.

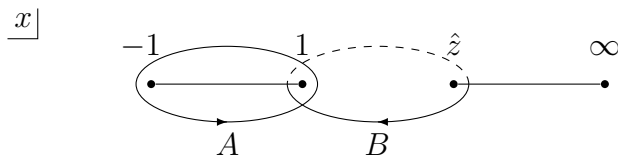


Figure 3:  $A$  and  $B$  cycles for the curve (4.39).

Specifically, let us take the branch cuts to be along  $[-1, 1]$  and  $[\hat{z}, \infty]$ , and take the  $A$ -cycle to go counterclockwise around the cut  $[-1, 1]$  and the  $B$ -cycle to go clockwise around  $[1, \hat{z}]$ . See Figure 3. Then the 2D harmonic functions can be chosen to be, with an arbitrary normalization,

$$g(z) = \frac{1}{\sqrt{2\pi}} \int_{-1}^1 \frac{dx}{\sqrt{(1-x^2)(\hat{z}-x)}} = \frac{\sqrt{2} \mathbf{K}(\frac{2}{\hat{z}+1})}{\pi \sqrt{\hat{z}+1}}, \quad (4.42a)$$

$$f(z) = \frac{i}{\sqrt{2\pi}} \int_1^{\hat{z}} \frac{dx}{\sqrt{(x^2-1)(\hat{z}-x)}} = \frac{i\sqrt{2} \mathbf{K}(\frac{\hat{z}-1}{\hat{z}+1})}{\pi \sqrt{\hat{z}+1}}, \quad (4.42b)$$

where  $\mathbf{K}(m)$  is the complete elliptic integral of the first kind.<sup>4</sup> We could multiply  $g, f$  by an overall factor. The monodromy of the cycles as we go counterclockwise around  $\hat{z} = 1$ , for example, is

$$B \rightarrow B, \quad A \rightarrow -2B + A, \quad (4.43)$$

where the base point is taken to be large positive  $\hat{z}$ . Correspondingly,  $f$  and  $g$  transform as

$$f \rightarrow f, \quad g \rightarrow -2f + g. \quad (4.44)$$

<sup>4</sup>We take the Mathematica convention for the argument of elliptic integrals.

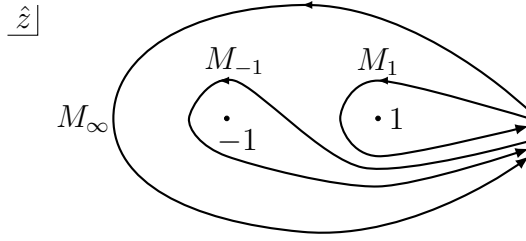


Figure 4: Paths to go around branes and monodromies

We represent this by the monodromy matrix

$$M_1 = \begin{pmatrix} 1 & 0 \\ -2 & 1 \end{pmatrix}, \quad M_{-1} = \begin{pmatrix} -1 & 2 \\ -2 & 3 \end{pmatrix}, \quad M_{\infty} = \begin{pmatrix} -1 & 2 \\ 0 & -1 \end{pmatrix}, \quad (4.45)$$

where we also presented the monodromy matrices for going counterclockwise around  $\hat{z} = -1, \infty$ . These satisfy  $M_1 M_{-1} = M_{\infty}$ . See Figure 4.

Let us find the 3D harmonic functions  $F, G$  that correspond to  $f, g$ . First, the large  $z$  expansion of  $g(z)$  is

$$g(z) = \frac{1}{\sqrt{2}} \sum_{k=0}^{\infty} \frac{a_{2k}}{\hat{z}^{2k+1/2}}, \quad (4.46)$$

where

$$a_{2k} = \frac{(4k)!}{2^{6k} (2k)! (k!)^2}, \quad a_0 = 1, \quad a_2 = \frac{3}{16}, \quad a_4 = \frac{105}{1024}, \quad a_6 = \frac{1155}{16384}, \quad \dots \quad (4.47)$$

This expansion can be derived by expanding the integrand of (4.42a) in  $1/\hat{z}$ . Applying the extension formula (3.17b) to this gives the 3D harmonic function

$$\begin{aligned} G(u, \sigma) &= \sqrt{\frac{u - \cos \sigma}{2Z}} \frac{1}{2\pi i} \oint_C \sum_{k=0}^{\infty} \frac{(2k)!}{(k!)^2} \frac{dt}{t - u} \left[ \frac{t^2 - 1}{8(t - u)Z} \right]^{2k} \\ &= \frac{\sqrt{2(u - \cos \sigma)Z}}{\pi} \oint \frac{dt}{\sqrt{(t^2 - 1)^2 - 16Z^2(t - u)^2}}, \end{aligned} \quad (4.48)$$

which is again an elliptic integral. Actually, it is more convenient to go to the  $w$  coordinate defined in (3.25). In terms of  $w$ , (4.48) can be written as a still another elliptic integral as

$$G = \frac{1}{2\sqrt{2}\pi} \sqrt{\frac{u - \cos \sigma}{Z}} \oint_A \frac{dw}{\sqrt{(w^2 - 1)(w^2 - \frac{u}{Z}w + \frac{1}{4Z^2})}} \quad (4.49)$$

where we chose  $a = 4$ . The contour  $A$  is chosen as in Figure 5. This choice of the contour is justified by noting that (4.49) reduces to (4.42a) in the scaling limit; this is straightforward

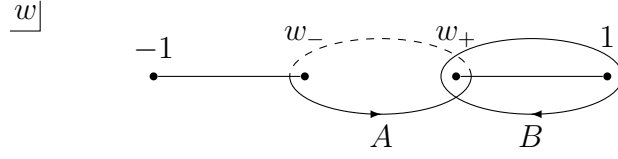


Figure 5: *Contours on the  $w$ -plane.*

to show by setting  $w = 1/x$  and taking the limit (3.20). With this choice of the contour, the integral (4.49) can be written as

$$\begin{aligned}
 G &= \frac{1}{\sqrt{2\pi}} \sqrt{\frac{u - \cos \sigma}{Z}} \int_{w_-}^{w_+} \frac{dt}{\sqrt{(w^2 - 1)(w^2 - \frac{u}{Z}w + \frac{1}{4Z^2})}} \\
 &= \frac{2\sqrt{2}}{\pi} \sqrt{\frac{(u - \cos \sigma)Z}{4Z^2 + 4Z\sqrt{u^2 - 1} - 1}} \mathbf{K}\left(\frac{8Z\sqrt{u^2 - 1}}{4Z^2 + 4Z\sqrt{u^2 - 1} - 1}\right). \quad (4.50)
 \end{aligned}$$

By expanding this in powers of  $1/Z$ , one can check that this reproduces the expansion (3.17a) with the Legendre function of the first kind,  $P_k(u)$ , multiplying  $Z^{-\frac{1}{2}-k}$ . It is manifest that this reduces to (4.42a) in the scaling limit.

The location of branes can be determined by finding the values of  $(u, \sigma)$  at which some of the branch points collide. This happens when  $w_+ = \pm 1$ ,<sup>5</sup> which gives

$$(u, \sigma) = (u_*, l), (u_*, l - \pi), \quad u_* \equiv \frac{1}{2} \left( \frac{2R}{|L|} + \frac{|L|}{2R} \right). \quad (4.51)$$

In the scaling limit (3.20) where  $u, |Z| \rightarrow \infty$ , this reproduces the position of branes in the 2D solution,  $\hat{z} = \pm 1$  (or  $z = \pm L$ ). As  $|Z| = \frac{R}{|L|}$  decreases,  $u_*$  decreases and the branes separate away from each other, until the singular limit  $|Z| = 1/2$  for which  $u_* = 1$  and they are on the  $x_3$ -axis. If we further decrease  $|Z|$ ,  $u_*$  increases again and, in the  $|Z| \rightarrow 0$  limit, the branes go back to  $u = \infty$ .

The other 3D harmonic function  $F$  cannot be obtained by the extension formula (3.17), because the large  $\hat{z}$  expansion of the 2D harmonic function  $f$  in (4.42b) contains  $\log \hat{z}$ :

$$f = \frac{i}{\sqrt{2\pi}} \sum_{k=0}^{\infty} \frac{a_{2k} \log(8\hat{z}) - b_{2k}}{\hat{z}^{\frac{1}{2}+2k}}, \quad b_0 = 0, \quad b_2 = \frac{5}{16}, \quad b_4 = \frac{389}{2048}, \quad b_6 = \frac{13327}{98304}, \quad \dots \quad (4.52)$$

where  $a_{2k}$  were defined (4.47). One way to circumvent this is to use the fact that, as we go around the brane at  $(u, \sigma) = (u_*, l)$ , the doublet  $(F, G)$  must undergo a monodromy by the matrix  $M_1$  in (4.45). Let  $B$  be the 1-cycle going clockwise around  $[w_+, 1]$  (see Figure 5). By examining how the branch points move as go around  $(u, \sigma) = (u_*, l)$ , we can show that the

<sup>5</sup>Here we assumed that  $|Z| > 1/2$ . If  $|Z| < 1/2$ , collision happens for  $w_- = \pm 1$ .

1-cycles  $A, B$  transform as just as (4.43). So,  $F$  is given by

$$\begin{aligned}
F(u, \sigma) &= \frac{1}{2\sqrt{2}\pi} \sqrt{\frac{u - \cos \sigma}{Z}} \oint_B \frac{dw}{\sqrt{(w^2 - 1)(w^2 - \frac{u}{Z}w + \frac{1}{4Z^2})}} \\
&= \frac{i}{\sqrt{2}\pi} \sqrt{\frac{u - \cos \sigma}{Z}} \int_{w_+}^1 \frac{dt}{\sqrt{(1 - w^2)(w^2 - \frac{u}{Z}w + \frac{1}{4Z^2})}} \\
&= \frac{2\sqrt{2}i}{\pi} \sqrt{\frac{(u - \cos \sigma)Z}{4Z^2 + 4Z\sqrt{u^2 - 1} - 1}} \mathbf{K} \left( \frac{4Z^2 - 4Z\sqrt{u^2 - 1} - 1}{4Z^2 + 4Z\sqrt{u^2 - 1} - 1} \right). \tag{4.53}
\end{aligned}$$

The large  $Z$  expansion of this is

$$\begin{aligned}
F &= \frac{i}{\sqrt{2}\pi} \sqrt{u - \cos \sigma} \sum_{k=0}^{\infty} \left( \frac{\log \frac{8Z}{\sqrt{u^2 - 1}}}{Z^{1/2}} + \frac{(3u^2 - 1) \log \frac{8Z}{\sqrt{u^2 - 1}} - (5u^2 - 1)}{16Z^{5/2}} \right. \\
&\quad \left. + \frac{2(105u^4 - 90u^2 + 9) \log \frac{8Z}{\sqrt{u^2 - 1}} - (389u^4 - 282u^2 + 21)}{2048Z^{9/2}} + \dots \right). \tag{4.54}
\end{aligned}$$

We can check that, in the scaling limit, this correctly reproduces the expansion (4.52). Or, more directly, we can see that the last expression of (4.53) reduces to (4.42b) in the scaling limit. One can confirm that, if we go around the other stack of branes at  $(u, \sigma) = (u_*, l - \pi)$ , corresponding to the  $\hat{z} = -1$  branes in the 2D limit, the 3D harmonic functions  $(F, G)$  correctly transform according to the monodromy matrix  $M_{-1}$  in (4.45). Therefore, the above  $(F, G)$  are the correct 3D extension of  $(f, g)$ . Being the periods of a  $w$ -torus, it is guaranteed that  $\tau = F/G$  has  $\text{Im } \tau > 0$ .

Note that, unlike  $G$ , this  $F$  diverges logarithmically at  $u = 1$ , namely on the  $x_3$ -axis. This implies that this solution is not just made of codimension-2 branes but also contains codimension-3 branes continuously distributed along the  $x_3$ -axis. This was not visible in the perturbative analysis in the previous work [20]. We can interpret this continuous distribution of charge as manifestation of the brane at  $\hat{z} = \infty$  in the 2D seed solution. We will study the charge distribution in detail below.

The fact that we have codimension-3 charge distributed on the  $x_3$ -axis is presumably related to the stability of the solution. In the 2D setting, the position of the branes are free parameters because the forces between branes cancel each other. However, when we go to 3D, the branes are bent and the balance of forces gets more nontrivial. It is possible that the charge sources on the  $x_3$  is necessary for the stability of the two circular branes.

In this solution, the source at infinity in the 2D seed is reappearing in the 3D setting in a different guise. This is unlike the ordinary supertube, for which the problem at the 2D infinity is resolved in the 3D solution. For the ordinary supertube, the 2D seed is  $g = 1, f = \frac{1}{2\pi i} \log \frac{z}{\mu}$ . This 2D solution does not make sense far away from the center,  $|z| > \mu$ , because  $\text{Im } \tau = \text{Im}(f/g)$  gets negative. However, the corresponding 3D solution is regular, even on

the  $x_3$ -axis, as discussed in Appendix B. We do not have a good understanding of why the ordinary supertube and the current example are different in this regard; we will discuss this matter further in section 5.

### 4.3.1 Charge distributions

From the explicit expression (4.50), one can straightforwardly show that the large  $r$  behavior of  $G$  is

$$G = \frac{Q_G}{r} + \dots, \quad Q_G = \sqrt{\frac{LR}{1 - \frac{L^2}{4R^2}}}. \quad (4.55)$$

$Q_G$  is the total  $G$  charge of the system. However, because of the nontrivial monodromies, it is not clear whether we can think of this charge as the sum of charges carried by the two separate stacks of branes or not. Moreover, the distribution of the charge for  $F$  is more non-trivial because of the aforementioned divergence on the  $x_3$ -axis. Here we study in detail the distribution of charges for  $G$  and  $F$ . Because the analysis is slightly lengthy, we present a summary at the end of this section on page 31.

As before, charges can be measured by integration over a Gaussian surface  $M^2$  as

$$Q_G = -\frac{1}{4\pi} \int_{M^2} *dG, \quad Q_F = -\frac{1}{4\pi} \int_{M^2} *dF. \quad (4.56)$$

In the present case,  $G, F$  are written as contour integrals on the  $w$ -plane as

$$G = \oint_A \omega, \quad F = \oint_B \omega, \quad (4.57)$$

where

$$\omega = \frac{1}{2\sqrt{2}\pi} \sqrt{\frac{u - \cos \sigma}{Z}} \frac{dw}{\sqrt{(w^2 - 1)(w^2 - \frac{u}{Z}w + \frac{1}{4Z^2})}} \quad (4.58)$$

is a 1-form on the  $w$ -plane and a scalar in  $\mathbb{R}^3$ . Since  $\omega$  is harmonic in  $\mathbb{R}^3$  as we discussed around (3.27), we can define  $\Omega$  by

$$*d\omega = d\Omega, \quad (4.59)$$

where  $d$  is the exterior derivative with respect to  $\mathbb{R}^3$ .  $\Omega$  is a 1-form on the  $w$ -plane and a 1-form in  $\mathbb{R}^3$ . Explicitly, in the present case,  $\Omega$  is given by

$$\Omega = \frac{iR}{2\sqrt{2}\pi} \frac{1}{\sqrt{(u - \cos \sigma)Z}} \frac{[(u - e^{i\sigma})w + \frac{1}{2Z}(e^{i\sigma} - 1)]dw}{(w - \frac{L}{2R})\sqrt{(w^2 - 1)(w^2 - \frac{u}{Z}w + \frac{1}{4Z^2})}} d\psi. \quad (4.60)$$

In terms of  $\Omega$ , we can write the charges as

$$Q_G = -\frac{1}{4\pi} \int_{\partial M^2} \oint_A \Omega, \quad Q_F = -\frac{1}{4\pi} \int_{\partial M^2} \oint_B \Omega. \quad (4.61)$$

We would like to use this expression to study the charge distribution. Although we wrote (4.61) as contour integrals along  $A$  and  $B$ , actually, the relevant contours change as we move in  $\mathbb{R}^3$ . Moreover, because  $\Omega$  has an additional pole at  $w = L/2R$  compared with  $\omega$ , we must specify whether or not we go around this pole. We will discuss these issues below.

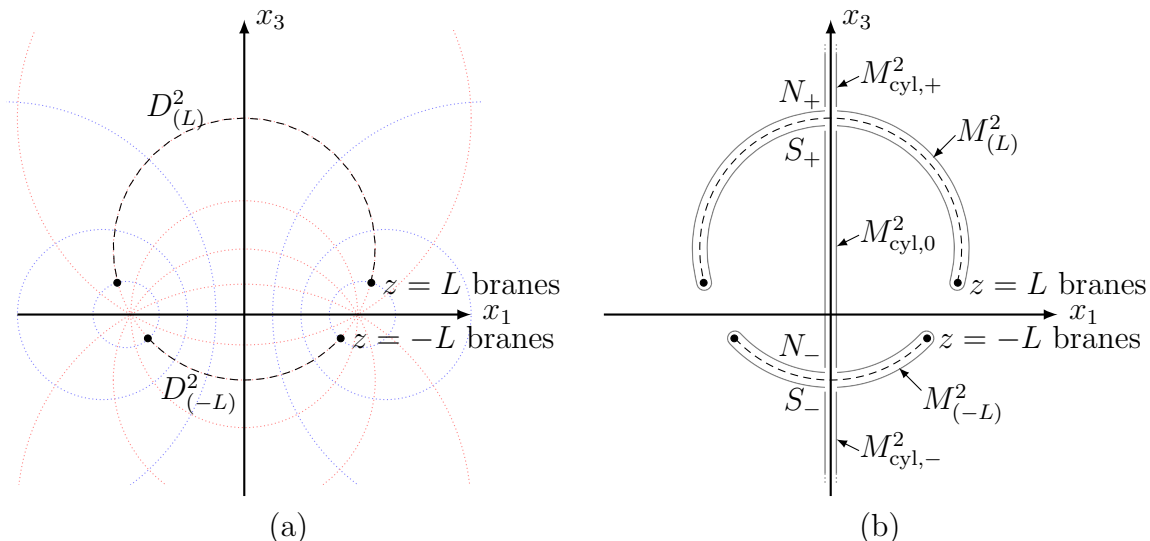


Figure 6: (a) The two stacks of branes in 3D (black blobs). The  $x_2 = 0$  cross section is shown; the actual branes are extending along circles whose center is on the  $x_3$ -axis. The stacks of branes that correspond to  $z = L, -L$  branes in 2D are at  $(u, \sigma) = (u_*, l), (u_*, l - \pi)$ , respectively, in 3D in the toroidal coordinates. We take the branch cuts for the monodromies around them to be constant- $\sigma$  surfaces  $D^2_{(\pm L)}$  shown by black dashed arcs. We also show some constant- $\sigma$  (red) and constant- $u$  (blue) curves by dotted lines. (b) Gaussian surfaces. We deform the Gaussian surface at infinity to the union  $M^2_{\text{cyl},+} \cup M^2_{(L)} \cup M^2_{\text{cyl},0} \cup M^2_{(-L)} \cup M^2_{\text{cyl},-}$  that avoids singular sources and branch cuts. See the text for more detail.

In view of the multi-valuedness of  $F$  and  $G$ , we deform the Gaussian surface  $M^2$  as follows. Consider 2-surfaces  $D^2_{(L)}$  and  $D^2_{(-L)}$  of disk topology, whose boundary is the branes at  $\sigma = l, l - \pi$ , respectively. We can choose  $D^2_{(\pm L)}$  arbitrarily but, to be specific, we take them to lie on constant- $\sigma$  surfaces (with  $\sigma = l, l - \pi$ ). So,

$$D^2_{(L)} = \{(u, \sigma = l) \mid u \leq u_*\}, \quad D^2_{(-L)} = \{(u, \sigma = l - \pi) \mid u \leq u_*\}; \quad (4.62)$$

see Figure 6(a). We take these to be the “branch cuts” across which the values of  $G, F$  jump. We cannot deform  $M^2$  past these branch cuts. So, we deform  $M^2$  into the union of the following Gaussian surfaces:

$$M^2_{\text{cyl},+} \cup M^2_{(L)} \cup M^2_{\text{cyl},0} \cup M^2_{(-L)} \cup M^2_{\text{cyl},-}. \quad (4.63)$$

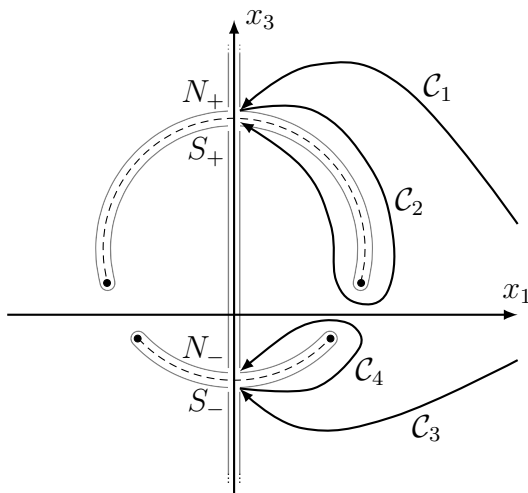


Figure 7: Paths in  $\mathbb{R}^3$  to reach Gaussian surfaces

Here, as shown in Figure 6(b),  $M_{\text{cyl},+}^2$  is a cylinder of a very small radius enclosing the  $x_3$ -axis above  $D_{(L)}^2$ ,  $M_{\text{cyl},-}^2$  is a cylinder below  $D_{(-L)}^2$ ,  $M_{\text{cyl},0}^2$  is a cylinder between  $D_{(L)}^2$  and  $D_{(-L)}^2$ , and  $M_{(\pm L)}^2$  is a surface that encloses  $D_{(\pm L)}^2$ . The boundaries of these surfaces are taken to be  $\psi$ -circles of a very small radius going around the  $x_3$ -axis, along which Dirac strings are. On these boundaries,  $u = 1$ . We will refer to the location of the boundary of  $M_{(L)}^2$  at its “north pole” (“south pole”) as  $N_+$  ( $S_+$ ), and the location of the boundary of  $M_{(-L)}^2$  at its “north pole” (“south pole”) as  $N_-$  ( $S_-$ ), as in Figure 6(b). Of course, where to take branch cuts is physically irrelevant.

We want to compute the charges contained in each of the Gaussian surfaces (4.63). To evaluate the last expression in (4.61), we only need the value of  $\Omega$  on the boundaries of the Gaussian surfaces where  $u = 1$ :

$$\Omega_\psi|_{u=1} = \frac{\sqrt{LR}}{2\pi} \text{sign}(\sin \frac{\sigma}{2}) \frac{dw}{(w - \frac{L}{2R})\sqrt{w^2 - 1}} \equiv \widehat{\Omega}. \quad (4.64)$$

We will be integrating this on the  $w$ -plane along a contour. In the  $u \rightarrow 1$  limit, the cut  $[w_+, w_-]$  around which contour  $A$  goes (see (3.28)) collapses to a point  $w = \frac{1}{2Z}$  and disappears. If contour  $A$  did not go around the pole at  $w = \frac{L}{2R}$ , then we would get zero for  $Q_G$ , which is inconsistent with (4.55). So, contour  $A$  must go around it. On the other hand, in the  $u \rightarrow 1$  limit, contour  $B$ , which is a closed path going around  $[w_-, 1]$  is equivalent to twice the open contour going from  $w = \frac{1}{2Z}$  to  $w = 1$  (twice because we go on the first and second sheets).

Let us start with the Gaussian surface  $M_{\text{cyl},\pm}^2$ . We can reach this region ( $N_+$  and  $S_-$ ) from the 3D infinity without changing the contour defining  $G, F$  (see the paths  $\mathcal{C}_1$  and  $\mathcal{C}_3$  in Figure 7). Rather than the charge enclosed by the entire  $M_{\text{cyl},\pm}^2$ , let us evaluate the charge

density by evaluating the charge in the infinitesimal interval  $[\sigma, \sigma + d\sigma]$ :

$$\begin{aligned} dQ_G &= -\frac{1}{2} d\sigma \frac{\partial}{\partial \sigma} \oint_A \widehat{\Omega} \\ &= -\text{sign}(\sin \frac{\sigma}{2}) \frac{\sqrt{LR}}{4\pi} d\sigma \frac{\partial}{\partial \sigma} \oint_{w=\frac{L}{2R}} \frac{dw}{(w - \frac{L}{2R})\sqrt{w^2 - 1}} = 0. \end{aligned} \quad (4.65)$$

This vanishes because nothing in the integral depends on  $\sigma$ . Therefore, there is no  $G$  charge on the  $x_3$ -axis, which we knew because  $G$  is regular there. For  $F$ , on the other hand, we get a nonvanishing result because the lower bound of the integral depends on  $\sigma$ :

$$\begin{aligned} dQ_F &= -\frac{1}{2} d\sigma \frac{\partial}{\partial \sigma} \oint_B \widehat{\Omega} \\ &= -\text{sign}(\sin \frac{\sigma}{2}) \frac{\sqrt{LR}}{2\pi} d\sigma \frac{\partial}{\partial \sigma} \int_{\frac{1}{2Z}}^1 \frac{dw}{(w - \frac{L}{2R})\sqrt{w^2 - 1}} \\ &= \frac{R}{2\pi} \frac{\sqrt{Z} d\sigma}{|\sin \frac{\sigma}{2}| \sqrt{1 - 4Z^2}} = \frac{iR dx_3}{2\pi \sqrt{(x_3 + iR)^2 - \frac{L^2}{4R^2}(x_3 - iR)^2}}, \end{aligned} \quad (4.66)$$

where in the last expression we wrote the density per unit length in  $x_3$ . We see that on the  $x_3$ -axis there is a nonvanishing density for  $Q_F$  that goes like  $\sim 1/x_3$ . Therefore, the total charge for  $F$  is not well defined in the sense that the total charge is only conditionally convergent.

Now we turn to  $M_{(L)}^2$  that encloses the  $z = L$  branes. This Gaussian surface has two boundaries at  $N_+$  and  $S_+$  (see Figure 6). Considering the orientation of the boundaries, the charge contained inside  $M_{(L)}^2$  is

$$Q_{G,F}|_{M_{(L)}^2} = -\frac{1}{2} \oint \widehat{\Omega}|_{N_+} + \frac{1}{2} \oint \widehat{\Omega}|_{S_+}. \quad (4.67)$$

The contours in the first term is the same as those for  $M_{\text{cyl},+}^2$  but, in the second term, the contours change as we go from  $N_+$  to  $S_+$  along the path  $\mathcal{C}_2$  in Figure 7. The change in the contours is given by the monodromy matrix  $M_1^{-1} = \begin{pmatrix} 1 & 0 \\ 2 & 1 \end{pmatrix}$  where  $M_1$  is given in (4.45). Therefore,

$$Q_G|_{M_{(L)}^2} = -\frac{1}{2} \oint_A \widehat{\Omega}|_{\sigma=l} + \frac{1}{2} \oint_{2B+A} \widehat{\Omega}|_{\sigma=l} = \oint_B \widehat{\Omega}|_{\sigma=l}, \quad (4.68)$$

$$Q_F|_{M_{(L)}^2} = -\frac{1}{2} \oint_B \widehat{\Omega}|_{\sigma=l} + \frac{1}{2} \oint_B \widehat{\Omega}|_{\sigma=l} = 0. \quad (4.69)$$

More explicitly,

$$Q_G|_{M_{(L)}^2} = \frac{\sqrt{LR}}{\pi} \int_{\frac{L}{2R}}^1 \frac{dw}{(w - \frac{L}{2R})\sqrt{w^2 - 1}}. \quad (4.70)$$

The analysis of  $M_{(-L)}^2$  that encloses the  $z = -L$  branes is similar to that of  $M_{(L)}^2$ . It has two boundaries at  $N_-$  and  $S_-$  (see Figure 6). The charge contained inside  $M_{(-L)}^2$  is

$$Q_{G,F}|_{M_{(-L)}^2} = -\frac{1}{2} \oint \widehat{\Omega}|_{N_-} + \frac{1}{2} \oint \widehat{\Omega}|_{S_-}. \quad (4.71)$$

The contours in the second term is the same as those for  $M_{\text{cycl},-}^2$  but, in the first term, the contours change as we go from  $S_-$  to  $N_-$  along the path  $\mathcal{C}_4$  in Figure 7. The change in the contours is given by the monodromy matrix  $M_{-1} = \begin{pmatrix} -1 & 2 \\ -2 & 3 \end{pmatrix}$  (see (4.45)). Therefore,

$$Q_G|_{M_{(-L)}^2} = -\frac{1}{2} \oint_{-2B+3A} \widehat{\Omega}|_{\sigma=l-\pi} + \frac{1}{2} \oint_A \widehat{\Omega}|_{\sigma=l-\pi} = \oint_{-A+B} \widehat{\Omega}|_{\sigma=l-\pi}, \quad (4.72)$$

$$Q_F|_{M_{(-L)}^2} = -\frac{1}{2} \oint_{-B+2A} \widehat{\Omega}|_{\sigma=l-\pi} + \frac{1}{2} \oint_B \widehat{\Omega}|_{\sigma=l-\pi} = \oint_{-A+B} \widehat{\Omega}|_{\sigma=l-\pi}. \quad (4.73)$$

Finally let us consider  $M_{\text{cycl},0}^2$ . We can reach it from 3D infinity by following the paths  $\mathcal{C}_1 \rightarrow \mathcal{C}_2$  or  $\mathcal{C}_3 \rightarrow \mathcal{C}_4$  in Figure 7. If we follow  $\mathcal{C}_1 \rightarrow \mathcal{C}_2$ , the charge inside  $M_{\text{cycl},0}^2$  is

$$Q_{F,G}|_{M_{\text{cycl},0}^2} = -\frac{1}{2} \oint \widehat{\Omega}|_{S_+} + \frac{1}{2} \oint \widehat{\Omega}|_{N_-}, \quad (4.74)$$

where the contours are just as for  $M_{(L)}^2$ . Therefore,

$$Q_G|_{M_{\text{cycl},0}^2} = -\frac{1}{2} \oint_{2B+A} \widehat{\Omega}|_{\sigma=l} + \frac{1}{2} \oint_{2B+A} \widehat{\Omega}|_{\sigma=l+\pi} = -\oint_B \widehat{\Omega}|_{\sigma=l} + \oint_B \widehat{\Omega}|_{\sigma=l+\pi}, \quad (4.75)$$

$$Q_F|_{M_{\text{cycl},0}^2} = -\frac{1}{2} \oint_B \widehat{\Omega}|_{\sigma=l} + \frac{1}{2} \oint_B \widehat{\Omega}|_{\sigma=l+\pi}, \quad (4.76)$$

where in the second equality of (4.75) we used the fact that the  $B$ -cycle integral of  $\widehat{\Omega}$  does not depend on  $\sigma \in [l, l+\pi]$  if  $0 < l < 2\pi$  (see (4.65)). The  $B$ -cycle integral does depend on  $\sigma$  and hence  $Q_G|_{M_{\text{cycl},0}^2}$  and  $Q_F|_{M_{\text{cycl},0}^2}$  are nonvanishing. Interestingly, although  $G$  has no charge source along the  $x_3$ -axis above or below the branes ( $M_{\text{cycl},\pm}^2$ ), it does have charge source in between ( $M_{\text{cycl},0}^2$ ).<sup>6</sup>

For  $G$ , there being no charge in  $M_{\text{cycl},\pm}^2$ , we can find the total charge  $Q_G$  by adding the contributions (4.68), (4.72) and (4.75) as

$$\begin{aligned} Q_G &= Q_G|_{M_{(L)}^2} + Q_G|_{M_{(-L)}^2} + Q_G|_{M_{\text{cycl},0}^2} \\ &= \oint_B \widehat{\Omega}|_{\sigma=l+\pi} + \oint_B \widehat{\Omega}|_{\sigma=l-\pi} - \oint_A \widehat{\Omega}|_{\sigma=l-\pi}. \end{aligned} \quad (4.77)$$

As is clear from (4.64),  $\widehat{\Omega}|_{\sigma=l+\pi} + \widehat{\Omega}|_{\sigma=l-\pi} = 0$ . Therefore,

$$\begin{aligned} Q_G &= -\oint_A \widehat{\Omega}|_{\sigma=l-\pi} \\ &= \frac{\sqrt{LR}}{2\pi} \oint_{w=\frac{L}{2R}} \frac{dw}{(w - \frac{L}{2R})\sqrt{w^2 - 1}} = \sqrt{\frac{LR}{1 - \frac{L^2}{4R^2}}}, \end{aligned} \quad (4.78)$$

which reproduces (4.55) as it should.

<sup>6</sup>However, this depends on where to put the branch cuts ( $D_{(\pm L)}^2$ ).

## Summary

Let us summarize the computation of charges above.

The multi-valuedness of the fluxes means that the charges are not carried only by the rings but also by the branch-cut disks whose boundaries are the rings. In addition, there is continuous distribution of charges on the  $x_3$ -axis. For the  $G$  charge, there is no charge on the  $x_3$ -axis above or below the branch-cut disks, but there is charge on part of the  $x_3$ -axis between the branch-cut disks. For the  $F$  charge, there is charge distribution on the entire  $x_3$ -axis. Because the  $F$  charge density decays as  $1/x_3$ , the total  $F$  charge is not well-defined. This means that, although this is a legitimate solution, it is difficult to regard it as a microstate of a black hole with definite charges.

Another observation is that the charges associated with individual rings satisfy

$$Q_G|_{M^2_{(L)}} = 0, \quad Q_G|_{M^2_{(-L)}} = Q_F|_{M^2_{(-L)}}. \quad (4.79)$$

This is what was already observed in the perturbative analysis in [20], and related to the fact that each stack of branes is a 1/2-BPS supertube. Concretely, the  $z = L$  and  $z = -L$  branes must come from the supertube transition of 1/4-BPS codimension-3 centers of charge vectors  $\Gamma_L = (a, (b, b, 0), (0, 0, a), 0)$  and  $\Gamma_{-L} = (a', (b', b', -a'), (b', b', a'), \frac{a'}{2})$ , respectively, where  $ab \neq 0, a'b' \neq 0$ . Because  $\langle \Gamma_L, \Gamma_{-L} \rangle = aa' + bb' \neq 0$ , this two-supertube configuration should be a bound state.

### 4.3.2 Absence of closed timelike curves

Let us see whether the solution contains CTCs along  $\psi$ . From (2.17) and (3.4), the  $\psi\psi$  component of the metric is proportional to

$$g_{\psi\psi} \propto -(u - \cos \sigma)^2 \omega_\psi^2 + R^2 (\text{Im}(F\bar{G}))^2 (u^2 - 1). \quad (4.80)$$

The 1-form  $\omega$  can be found by solving (2.18). Assuming that  $\omega$  is independent of  $\psi$ , we find that  $\omega_\sigma = \omega_u = 0$  and that  $\omega_\psi$  satisfies

$$\partial_u \omega_\psi = -\frac{R}{u - \cos \sigma} \text{Re}(F\partial_\sigma \bar{G} - G\partial_\sigma \bar{F}), \quad \partial_\sigma \omega_\psi = \frac{R(u^2 - 1)}{u - \cos \sigma} \text{Re}(F\partial_u \bar{G} - G\partial_u \bar{F}). \quad (4.81)$$

First, let us look at the region near the  $x_3$ -axis where we have a continuous distribution of charges, by setting  $u = 1 + \epsilon$  and expanding various quantities in  $\epsilon$ . Using the explicit expressions (4.50), (4.53), we find

$$F\partial_u \bar{G} - \bar{G}\partial_u F = \frac{iC}{\epsilon} + A + B \log \epsilon + \dots, \quad C = \frac{Z_0(1 - \cos \sigma)}{\pi |4e^{2i(\sigma-l)} Z_0^2 - 1|}, \quad (4.82)$$

where  $Z = Z_0 e^{i(\sigma-l)}$ ,  $Z_0 = \frac{R}{|L|}$ .  $A$  and  $B$  are some complex quantities that depend on  $\sigma$ . Therefore, the second equation in (4.81) gives

$$\partial_\sigma \omega_\psi \sim \epsilon \operatorname{Re}(F \partial_u \bar{G} - \bar{G} \partial_u F) \sim A' \epsilon + B' \epsilon \log \epsilon + (\text{higher order in } \epsilon), \quad (4.83)$$

where  $A', B'$  are some real quantities that depend on  $\sigma$ . Note that the  $\mathcal{O}(1/\epsilon)$  term in (4.82) has dropped out. Integrating this with respect to  $\sigma$ , we get

$$\omega_\psi \sim \epsilon A'' + B'' \epsilon \log \epsilon + \dots. \quad (4.84)$$

“...” here contain an integration constant which is independent of  $\sigma$  but can depend on  $\epsilon$ . However, if we require that  $\omega$  vanish at 3D infinity ( $\epsilon = 0$ ), then such a constant must also vanish as  $\epsilon \rightarrow 0$ . So, “...” here are higher order in  $\epsilon$ , or can be absorbed in  $A'', B''$ . On the other hand, we find

$$F \bar{G} = iC \log \frac{1}{\epsilon} + \dots. \quad (4.85)$$

Therefore, (4.80) becomes

$$g_{\psi\psi} \sim -\epsilon^2 (A'' + B'' \log \epsilon)^2 + \epsilon C^2 (\log \epsilon)^2, \quad (4.86)$$

which is positive for small  $\epsilon \rightarrow 0$ . So, there is no CTC near the  $x_3$ -axis.

Next, let us look at the region near the branes. Let us focus on the region near the stack of branes at  $(u, \sigma) = (u_*, l)$ , by setting

$$u = u_* + \Delta u, \quad \sigma = l + \Delta \sigma, \quad u_* = Z_0 + \frac{1}{4Z_0}, \quad (4.87)$$

and expanding various quantities in  $\Delta u, \Delta \sigma$ . We find

$$F \partial_\sigma \bar{G} - \bar{G} \partial_\sigma F = \frac{1 + 4Z_0^2 - 4Z_0 \cos l}{4\pi(4Z_0 \Delta u + i(4Z_0^2 - 1)\Delta \sigma)} + \dots. \quad (4.88)$$

Plugging this into the first equation of (4.81), we find

$$\omega_\psi = -\frac{R(1 + 4Z_0^2 - 4Z_0 \cos l)}{16\pi Z_0(u_* - \cos l)} \log r_\perp + \dots, \quad (4.89)$$

where

$$r_\perp = \frac{R}{u_* - \cos l} \sqrt{\frac{(\Delta u)^2}{u_*^2 - 1} + (\Delta \sigma)^2} \quad (4.90)$$

is the distance from the location of the brane. On the other hand,

$$\operatorname{Im}(F \bar{G}) = \frac{1 + 4Z_0^2 - 4Z_0 \cos l}{4\pi(4Z_0^2 - 1)} \log r_\perp + \dots. \quad (4.91)$$

If we plug (4.89) and (4.91) into (4.80), we find that the two contributions cancel:

$$g_{\psi\psi} = 0 \cdot (\log r_{\perp})^2 + \dots \quad (4.92)$$

So, the  $\psi$  direction is null at the leading order. This is consistent with the fact that, up to U-duality, each stack of branes is just an ordinary supertube along which the metric becomes null [23]. The subleading terms in (4.92) cannot be determined in this local analysis because we do not know the constant of integration in (4.89), which is determined by the boundary condition at the other end of space, that  $\omega = 0$  at  $u = 1$ . However, physically we expect that there is no CTC much as for ordinary supertubes.

## 5 Discussions

In this paper, we constructed examples of exact solutions that represent non-Abelian supertubes in the framework of the multi-center solutions. Multi-center solutions are characterized by 3D harmonic functions, and supertubes correspond to codimension-2 singularities in the harmonic functions. In order to construct desired 3D harmonic functions, we started with 2D harmonic functions that represent F-theory-like configurations of branes in a 2D  $z$ -plane. We extended those 2D harmonic functions to 3D harmonic functions, by an extension formula, which essentially replaces  $z^{-k}$  in 2D by a Legendre function  $P_{k-\frac{1}{2}}(u)$ .

We worked out two explicit examples in the main text. In the first example, we took as a 2D seed the constant- $\tau$  solution with a single stack of branes. The resulting 3D solution contains a single circular stack of codimension-2 branes, around which there is a non-trivial monodromy. If the number of branes is  $N \leq 6$ , the solution is free from physical issues such as CTCs and can be thought of as a new microstate of a black hole with a finite entropy in  $\text{AdS}_2 \times S^2$ . This example is perhaps a little too simple having only one ring. As a next example, we considered a solution that has two stacks of circular branes with non-Abelian monodromies. This solution has no CTCs and has a curious feature that there is continuous distribution of charges on the  $x_3$ -axis. We gave a detailed analysis of the charges in this configuration, and found that the charge density on the  $x_3$ -axis makes it difficult to interpret this solution as a microstate of a black hole. This extra charge presumably necessary for the stability of the configuration. In Appendix C, we considered more examples, but they have a serious problem of the monodromy in the 3D solution being different from that in the 2D solution that we started with.

Thus we have made important steps toward constructing general black-hole microstates involving codimension-2 centers. However, the above issues must be clarified in order to construct more general solutions.

Let us discuss points potentially relevant to these issues. We used the extension formula (3.17) to extend 2D seed solutions to 3D solutions, but this procedure leaves some ambigu-

ties. The extension formula essentially replaces  $z^{-k}$  in 2D by the Legendre function  $P_{k-\frac{1}{2}}(u)$ . However, we are free to include the other Legendre function  $Q_{k-\frac{1}{2}}(u)$ , because it does not spoil the matching. Furthermore, there is freedom to change the coefficient of  $z^{-k}$  by a number that vanishes in the scaling limit. To appreciate these points, let us look at the 3D harmonic function  $F$  that we studied in the two-stack example in section 4.3. We applied the extension formula to the 2D harmonic function  $g$  to construct the 3D harmonic function  $G$ , while  $F$  was obtained from  $G$  by the monodromy requirement, without using the extension formula. The large  $Z$  expansion of  $F$  (4.54) can be written as

$$F = \frac{i}{\sqrt{2\pi}} \sqrt{u - \cos \sigma} f, \quad f = f_{-1/2} Z^{-1/2} + f_{-5/2} Z^{-5/2} + \dots, \quad (5.1)$$

where

$$\begin{aligned} f_{-1/2} &= -(\mathcal{P}_0 - i\sigma P_0) + P_0 \log \frac{4R}{L} + Q_0, \\ f_{-5/2} &= \frac{1}{8} \left[ -(\mathcal{P}_2 - i\sigma P_2) + \log \frac{4R}{L} P_2 + Q_2 \right] - \frac{1}{16} P_2, \\ f_{-9/2} &= \frac{3}{128} \left[ -(\mathcal{P}_4 - i\sigma P_4) + \log \frac{4R}{L} P_4 + Q_4 \right] - \frac{7}{512} P_4, \quad \dots \end{aligned} \quad (5.2)$$

We saw that, in the scaling limit, this  $F$  reproduces the 2D harmonic function  $f$  (4.52). However, (5.2) also contains  $Q_k(u)$ , which cannot be obtained by the extension formula. We have another ambiguity in constructing 3D harmonic functions from 2D ones. Because the 2D seed is holomorphic, we assumed that the 3D harmonic functions are also “holomorphic” in the sense discussed below (3.27) or (A.24). However, as far as matching is concerned, we could have also included “antiholomorphic” pieces as long as they do not contribute in the scaling limit. An interesting example in this regard is the ordinary supertube solution discussed in Appendix B. In that solution, the harmonic functions involve only  $Q, \mathcal{Q}$  and not  $P, \mathcal{P}$ . Furthermore, that harmonic functions do not just have holomorphic parts but also antiholomorphic pieces that do not contribute in the scaling limit. The structure of the harmonic functions, including the antiholomorphic part, is determined by the monodromy requirement. These examples may mean that, although there are ambiguities in constructing 3D harmonic functions, the requirement of desired monodromies is strong enough to completely fix those ambiguities. This matter certainly deserves further investigation. In particular, it is important to clarify whether or not the charge distribution on the  $x_3$ -axis of the two-stack example is an unavoidable consequence of the monodromy requirement.

It is possible that the class of solutions we studied in the current paper is too restrictive. We focused on the so-called SWIP solutions where the moduli  $\tau_1, \tau_2$  are fixed to  $i$ . This is not a very mild assumption; for example, it excludes 1/2-BPS primitive centers of codimension 3, which are crucial for the construction of the bubbling microstate geometries [6, 7]. It is desirable to study more general solutions with one or both of  $\tau_1$  and  $\tau_2$  are allowed to vary.

Allowing one to vary may be manageable, because the eight harmonic functions can be written in terms of two pairs of complex functions each of which transforms under  $SL(2, \mathbb{Z})$  [20, Appendix C].

Another direction is to include both codimension-2 centers and codimension-3 centers from the start [19]. In particular, our second example suggests that having codimension-2 centers with non-commuting monodromies is not generally stable on its own. By explicitly including codimension-3 centers, we can hope to find simple solutions representing genuine microstates of black holes. As mentioned above, for the additional codimension-3 center to be 1/2-BPS primitive, we must go out of the SWIP class of solutions.

## Acknowledgments

We would like to thank Iosif Bena and Kazumi Okuyama for discussions. We thank José J. Fernández-Melgarejo and Minkyu Park, and Hitoshi Sakai for collaboration in the early stages of the project. The work of MS was supported in part by MEXT KAKENHI Grant Numbers 21K03552 and 21H0518.

## A Legendre functions and resonant Legendre functions

### A.1 Legendre functions

The Legendre functions are solutions of the Legendre differential equation

$$(1 - z^2)f'' - 2zf' + \nu(\nu + 1)f = 0, \quad \nu \in \mathbb{C}. \quad (\text{A.1})$$

The Legendre function of the first kind can be defined by the so-called Schläfli integral

$$P_\nu(z) = \frac{1}{2\pi i} \oint_C \frac{dt}{t - z} \left[ \frac{t^2 - 1}{2(t - z)} \right]^\nu. \quad (\text{A.2})$$

For general  $\nu$ , the integrand has logarithmic branch cuts which are taken to be the intervals  $[-\infty, -1]$  and  $[1, z]$ . The contour  $C$  goes counterclockwise around the branch cut  $[1, z]$ . The phase is chosen so that  $\arg\left(\frac{t^2-1}{t-z}\right) \rightarrow 0$  for sufficiently large  $t > 0$ . Thus defined  $P_\nu(z)$  is single-valued on a  $z$ -plane with a cut along  $[-\infty, -1]$  and satisfies  $P_\nu(1) = 1$ .

There are multiple ways to define the Legendre function of the second kind,  $Q_\nu(z)$ , which is an independent solution of the Legendre differential equation. Here we define it as

$$Q_\nu(z) = \frac{1}{4i \sin \pi \nu} \oint_C \frac{dt}{z - t} \left[ \frac{t^2 - 1}{2(z - t)} \right]^\nu, \quad \nu \in \mathbb{C}, \quad (\text{A.3})$$

with the following contour:

$$(A.4)$$

The phase of the integrand is chosen so that  $\arg(t^2 - 1) = 0$  at point P and  $\arg(z - t) = \arg z$  at  $t = 0$ . Thus defined  $Q_\nu(z)$  has a branch cut along  $[-\infty, 1]$  and defined for all  $\nu \in \mathbb{C}$  except for  $\nu = -1, -2, \dots$ . In Mathematica, this  $Q_\nu(z)$  is called the Legendre function of the second kind of type 3. For  $\text{Re}(1 + \nu) > 1$ , this  $Q_\nu(z)$  can be rewritten as

$$Q_\nu(z) = \frac{1}{2} \int_{-1}^1 \frac{(1 - t^2)^\nu}{2^\nu (z - t)^{\nu+1}} dt. \quad (A.5)$$

The explicit expressions for some small values of  $\nu$  are

$$\begin{aligned} P_0(z) &= 1, & P_1(z) &= z, & P_2(z) &= \frac{1}{2}(3z^2 - 1), \\ Q_0(z) &= \frac{1}{2} \log \frac{z+1}{z-1}, & Q_1(z) &= \frac{1}{2} P_1(z) \log \frac{z+1}{z-1} - 1, \\ Q_2(z) &= \frac{1}{2} P_2(z) \log \frac{z+1}{z-1} - \frac{3z}{2}. \end{aligned} \quad (A.6)$$

Because the Legendre equation (A.1) is unchanged under  $\nu \rightarrow -\nu - 1$ , the Legendre functions  $(P_{\nu-1/2}, Q_{\nu-1/2})$  are linear combinations of  $(P_{-\nu-1/2}, Q_{-\nu-1/2})$ . Indeed,  $P_\nu(z)$  satisfies

$$P_{\nu-1/2}(z) = P_{-\nu-1/2}(z), \quad \nu \in \mathbb{C}, \quad (A.7)$$

while  $Q_\nu(z)$  satisfies

$$Q_{m-1/2}(z) = Q_{-m-1/2}(z), \quad m \in \mathbb{Z}. \quad (A.8)$$

The behavior near  $z = 1$  is

$$P_\nu(z) = 1 + \frac{\nu(1+\nu)}{2}(z-1) + \dots, \quad (A.9a)$$

$$Q_\nu(z) = -\frac{1}{2} \log \frac{z-1}{2} - (\psi(\nu+1) + \gamma) + \dots, \quad (A.9b)$$

where  $\psi(z)$  is the digamma function and  $\gamma$  is the Euler-Mascheroni constant. The behavior near  $z = \infty$  is, for generic  $\nu \notin \mathbb{Z}/2$ ,

$$\begin{aligned} P_\nu(z) &= \frac{2^{-\nu-1} \Gamma(-\nu - 1/2)}{\sqrt{\pi} \Gamma(-\nu)} (z-1)^{-\nu-1} \left( 1 - \frac{\nu+1}{z-1} + \dots \right) \\ &+ \frac{2^\nu \Gamma(\nu+1/2)}{\sqrt{\pi} \Gamma(\nu+1)} (z-1)^\nu \left( 1 + \frac{\nu}{z-1} + \dots \right). \end{aligned} \quad (A.10)$$

If  $\nu \in \mathbb{R}$  and  $\nu \notin \mathbb{Z} + \frac{1}{2}$ ,

$$P_\nu(z) = \begin{cases} \frac{\Gamma(2\nu+1)}{2^\nu \Gamma(\nu+1)^2} z^\nu + \dots & (\nu > -\frac{1}{2}) \\ \frac{2^{\nu+1} \Gamma(-2\nu-1)}{\Gamma(-\nu)^2} z^{-\nu-1} + \dots & (\nu < -\frac{1}{2}) \end{cases} \quad (\text{A.11})$$

So, as  $z \rightarrow \infty$ ,  $P_\nu(u)$  diverges for  $|\nu - 1/2| > 0$  and vanishes for  $|\nu - 1/2| < 0$ . The expansion for  $Q_\nu(z)$  for generic  $\nu$  is

$$Q_\nu(z) = \frac{2^{-\nu-1} \sqrt{\pi} \Gamma(\nu+1)}{\Gamma(\nu+3/2)} z^{-\nu-1} \left[ 1 + \frac{(1+\nu)(2+\nu)}{2(3+2\nu)z^2} + \dots \right]. \quad (\text{A.12})$$

For  $\nu > -1$ , this vanishes as  $z \rightarrow \infty$  while, for generic  $\nu < -1$ , it diverges as  $z \rightarrow \infty$ .

By the coordinate transformation (3.25) with  $a = 2$ ,  $P_\nu(z)$  can be written as

$$P_\nu(z) = \frac{1}{2\pi i} \oint_C \frac{w^\nu dw}{\sqrt{w^2 - 2zw + 1}} = \frac{1}{\pi} \int_{w_-}^{w_+} \frac{w^\nu dw}{\sqrt{-w^2 + 2zw - 1}} \quad (\text{A.13})$$

where in the first expression the contour goes counterclockwise around the cut  $[w_-, w_+]$ ,  $w_\pm = u \pm \sqrt{u^2 - 1}$ , and the phase is taken so that  $\arg(w^2 - 2zw + 1) = 0$  for positive  $w > w_+$ . Likewise,  $Q_\nu(z)$  can be written as

$$Q_\nu(z) = \int_0^{w_-} \frac{w^\nu dw}{\sqrt{w^2 - 2zw + 1}}. \quad (\text{A.14})$$

We could define this as a contour integral along a Pochhammer contour going around  $w = 0, w_-$ .

## A.2 Resonant Legendre functions

The resonant Legendre equation [33] is the Legendre equation (A.1) with a inhomogeneous term proportional to the Legendre function. Here we consider the following equation in particular:

$$(1 - z^2)\mathcal{P}_\nu''(z) - 2z\mathcal{P}_\nu'(z) + \nu(\nu+1)\mathcal{P}_\nu(z) = -(2\nu+1)P_\nu(z). \quad (\text{A.15})$$

By differentiating the Legendre differential equation (A.1) with respect to  $\nu$ , we immediately see that the solution  $\mathcal{P}_\nu(z)$  is nothing but the  $\nu$ -derivative of  $P_\nu(z)$ :

$$\mathcal{P}_\nu(z) = \partial_\nu P_\nu(z) = \frac{1}{2\pi i} \oint_C \frac{w^\nu \log w dw}{\sqrt{1 - 2zw + w^2}} = \frac{1}{\pi} \int_{w_-}^{w_+} \frac{w^\nu \log w dw}{\sqrt{-1 + 2zw - w^2}}, \quad (\text{A.16})$$

where we used (A.13). Similarly, we can define  $\mathcal{Q}_\nu(z)$  as the solution to the differential equation (A.15) with  $P_\nu(z)$  on the right hand side replaced by  $Q_\nu(z)$ . From (A.14), we see that it can be written as

$$\mathcal{Q}_\nu(z) = \partial_\nu Q_\nu(z) = \int_0^{w_-} \frac{w^\nu \log w dw}{\sqrt{w^2 - 2zw + 1}}. \quad (\text{A.17})$$

The explicit expressions for some small values of  $\nu$  are

$$\begin{aligned}
\mathcal{P}_0(z) &= \log \frac{z+1}{2}, & \mathcal{P}_1(z) &= z \log \frac{z+1}{2} + z - 1, \\
\mathcal{P}_2(z) &= P_2(z) \log \frac{z+1}{2} + \frac{7}{4}z^2 - \frac{3}{2}z - \frac{1}{4}, \\
\mathcal{Q}_0(z) &= -\frac{1}{2} \log \frac{z+1}{2} \log \frac{z-1}{2} - \text{Li}_2 \frac{1-z}{2} - \frac{\pi^2}{6}, \\
\mathcal{Q}_1(z) &= z\mathcal{Q}_0(z) + \frac{z+1}{2} \log \frac{z+1}{2} - \frac{z-1}{2} \log \frac{z-1}{2} + 1, \\
\mathcal{Q}_2(z) &= P_2(z)\mathcal{Q}_0(z) + \left(-\frac{7z^2}{8} + \frac{3z}{4} + \frac{1}{8}\right) \log \left(\frac{z-1}{2}\right) \\
&\quad + \left(\frac{7z^2}{8} + \frac{3z}{4} - \frac{1}{8}\right) \log \left(\frac{z+1}{2}\right) + \frac{5z}{4}.
\end{aligned} \tag{A.18}$$

For  $\nu = -1/2$ , the resonant Legendre equation is the same as the Legendre equation and therefore the former must be expressible in terms of the latter. Indeed,

$$\begin{aligned}
\mathcal{P}_{-1/2}(z) &= 0, \\
\mathcal{Q}_{-1/2}(z) &= -\frac{\pi^2}{2} P_{-1/2}(z) = -\pi \mathbf{K}\left(\frac{1-z}{2}\right),
\end{aligned} \tag{A.19}$$

where  $\mathbf{K}(m)$  is the complete elliptic integral of the first kind.

The values at  $z = 1$  are

$$\mathcal{P}_\nu(z=1) = 0, \quad \mathcal{Q}_\nu(z=1) = -\psi^{(1)}(1+\nu), \tag{A.20}$$

where  $\psi^{(m)}(x)$  is the polygamma function.

The behavior as  $z \rightarrow \infty$  is, for  $\nu \in \mathbb{R}$  and  $\nu \notin \mathbb{Z} + \frac{1}{2}$ ,

$$\mathcal{P}_\nu(z) = \begin{cases} \frac{\Gamma(2\nu+1)}{2^\nu \Gamma(\nu+1)^2} z^\nu \log z + \dots & (\nu > -\frac{1}{2}) \\ -\frac{2^{\nu+1} \Gamma(-2\nu-1)}{\Gamma(-\nu)^2} z^{-\nu-1} \log z + \dots & (\nu < -\frac{1}{2}) \end{cases} \tag{A.21}$$

The behavior of  $\mathcal{Q}_\nu(z)$  as  $z \rightarrow \infty$  is, for generic  $\nu$ ,

$$\mathcal{Q}_\nu(z) = -\frac{2^{-\nu-1} \sqrt{\pi} \Gamma(\nu+1)}{\Gamma(\nu+3/2)} z^{-\nu-1} \log z + \dots \tag{A.22}$$

For  $\nu > -1$ , this vanishes as  $z \rightarrow \infty$  while, for generic  $\nu < -1$ , it diverges as  $z \rightarrow \infty$ .

### A.3 Relation to harmonic functions

As discussed in the main text,

$$\sqrt{u - \cos \sigma} e^{\pm i(\nu + \frac{1}{2})\sigma} P_\nu(u), \quad \sqrt{u - \cos \sigma} e^{\pm i(\nu + \frac{1}{2})\sigma} Q_\nu(u) \tag{A.23}$$

are harmonic functions in 3D. If  $\nu > -\frac{1}{2}$  and  $\nu \notin \mathbb{Z} + \frac{1}{2}$ , the  $u \rightarrow \infty$  behavior is, from (A.11),

$$\sqrt{u - \cos \sigma} e^{\pm i(\nu + \frac{1}{2})\sigma} P_\nu(u) \sim (e^{\pm i\sigma} u)^{\nu + \frac{1}{2}} \propto \begin{cases} \bar{z}^{-\nu - \frac{1}{2}} \\ z^{-\nu - \frac{1}{2}} \end{cases}, \quad (\text{A.24a})$$

$$\sqrt{u - \cos \sigma} e^{\pm i(\nu + \frac{1}{2})\sigma} Q_\nu(u) \sim \left(\frac{e^{\pm i\sigma}}{u}\right)^{\nu + \frac{1}{2}} \propto \begin{cases} z^{\nu + \frac{1}{2}} \\ \bar{z}^{\nu + \frac{1}{2}} \end{cases}, \quad (\text{A.24b})$$

where we also wrote down the corresponding 2D functions using the identification  $z \propto e^{i\sigma}/u$  (Eq. (3.13)). (A.24a) corresponds to (anti)holomorphic functions that diverge near the 2D infinity, while (A.24b) corresponds to (anti)holomorphic functions that vanish near the 2D infinity.

As discussed in (3.11), the combinations

$$\begin{aligned} & \sqrt{u - \cos \sigma} e^{\pm i(\nu + \frac{1}{2})\sigma} (\mathcal{P}_\nu(u) \pm i\sigma P_\nu(u)), \\ & \sqrt{u - \cos \sigma} e^{\pm i(\nu + \frac{1}{2})\sigma} (\mathcal{Q}_\nu(u) \pm i\sigma Q_\nu(u)) \end{aligned} \quad (\text{A.25})$$

are also harmonic functions in 3D. Another way to see the harmonicity is as follows. Using the integral expressions (A.13), (A.16), this can be rewritten as

$$\begin{aligned} & \sqrt{u - \cos \sigma} e^{\pm i(\nu + \frac{1}{2})\sigma} (\mathcal{P}_\nu(u) \pm i\sigma P_\nu(u)) \\ &= \sqrt{u - \cos \sigma} e^{\pm i\sigma/2} \frac{1}{2\pi i} \oint \frac{(we^{\pm i\sigma})^\nu \log(we^{\pm i\sigma}) dw}{\sqrt{w^2 - 2uw + 1}} \\ &= \sqrt{u - \cos \sigma} e^{\pm i\sigma/2} \frac{1}{2\pi i} \oint \frac{w'^\nu \log w' dw'}{\sqrt{w'^2 - 2uw' e^{\pm i\sigma} + e^{\pm 2i\sigma}}} \end{aligned} \quad (\text{A.26})$$

where we set  $we^{\pm i\sigma} = w'$ . This is harmonic, because the Laplacian of

$$\sqrt{u - \cos \sigma} e^{\pm i\sigma/2} \frac{1}{\sqrt{w'^2 - 2uw' e^{\pm i\sigma} + e^{\pm 2i\sigma}}} \quad (\text{A.27})$$

identically vanishes for any  $w'$ . The same is true for the combination of  $Q, \mathcal{Q}$  in (A.25).

The behavior of (A.25) as  $u \rightarrow \infty$  for  $\nu > \frac{1}{2}$  and  $\nu \notin \mathbb{Z} + \frac{1}{2}$  is, from (A.21) and (A.22),

$$\sqrt{u - \cos \sigma} e^{\pm i(\nu + \frac{1}{2})\sigma} (\mathcal{P}_\nu(u) \pm i\sigma P_\nu(u)) \sim (e^{\pm i\sigma} u)^{\nu + \frac{1}{2}} \log(e^{\pm i\sigma} u) \sim \begin{cases} \bar{z}^{-\nu - \frac{1}{2}} \log \bar{z} \\ z^{-\nu - \frac{1}{2}} \log z \end{cases}, \quad (\text{A.28a})$$

$$\sqrt{u - \cos \sigma} e^{\pm i(\nu + \frac{1}{2})\sigma} (\mathcal{Q}_\nu(u) \pm i\sigma Q_\nu(u)) \sim \left(\frac{e^{\pm i\sigma}}{u}\right)^{\nu + \frac{1}{2}} \log\left(\frac{e^{\pm i\sigma}}{u}\right) \sim \begin{cases} z^{\nu + \frac{1}{2}} \log z \\ \bar{z}^{\nu + \frac{1}{2}} \log \bar{z} \end{cases}. \quad (\text{A.28b})$$

## B The ordinary supertube

In the main text, we studied 3D solutions by extending 2D solutions that involve multiple stacks of branes with non-Abelian monodromies (the constant- $\tau$  solutions are regarded as

multiple stacks with non-Abelian monodromies collapsing to a point). However, a simpler possibility is to start with the 2D solution corresponding to a single brane,

$$f = \frac{1}{2\pi i} \log \frac{z}{\mu}, \quad g = 1, \quad (\text{B.1})$$

where  $\mu$  is a constant. As we go around  $z = 0$ , this solution has the monodromy

$$\begin{pmatrix} f \\ g \end{pmatrix} \rightarrow \begin{pmatrix} 1 & 1 \\ 0 & 1 \end{pmatrix} \begin{pmatrix} f \\ g \end{pmatrix}. \quad (\text{B.2})$$

The 2D solution (B.1) physically makes sense only near the origin; for  $|z| > \mu$ ,  $\text{Im} \tau = \text{Im}(f/g) = \frac{1}{2\pi} \log \frac{\mu}{|z|}$  gets negative and the solution is not acceptable. The point of F-theory is to resolve this problem at long distance by including other branes with non-commuting monodromies. However, if we extend (B.1) to 3D, it is possible that this is resolved by a different long distance effect, namely, the infinitely long straight brane in 2D is actually a closed circle in 3D.

Indeed, the 3D solution that reduces to (B.1) in the 2D limit is just the ordinary supertube and the harmonic functions are given by [25]

$$F = \gamma + i\varphi, \quad G = 1, \quad (\text{B.3})$$

where

$$\varphi(u, \sigma) = \frac{1}{2\sqrt{2}} \sqrt{u - \cos \sigma} P_{-1/2}(u), \quad (\text{B.4})$$

$$\gamma(u, \sigma) = \frac{1}{R} \left[ \frac{a(u)}{\sqrt{u-1}} \mathbf{F}\left(\frac{\sigma}{2} \middle| -\frac{2}{u-1}\right) - 2\sqrt{u-1} a'(u) \mathbf{E}\left(\frac{\sigma}{2} \middle| -\frac{2}{u-1}\right) \right], \quad (\text{B.5})$$

$$a(u) = -\frac{R}{8\sqrt{2}} \frac{u^2 - 1}{u^{3/2}} {}_2F_1\left(\frac{3}{4}, \frac{5}{4}; 2; 1 - u^{-2}\right). \quad (\text{B.6})$$

Here,  $\mathbf{F}(\phi|m)$  and  $\mathbf{E}(\phi|m)$  are the elliptic integrals of the first and second kinds, respectively. This solution has  $\text{Im} \tau = \varphi(u, \sigma) > 0$  everywhere and has the monodromy (B.2) because

$$\gamma(u, \sigma) \rightarrow \gamma(u, \sigma) + 1 \quad \text{as} \quad \sigma \rightarrow \sigma + 2\pi, \quad (\text{B.7})$$

as can be shown from the properties of the elliptic integrals. Furthermore, the  $u \rightarrow \infty$  behavior is

$$\begin{aligned} \gamma &= \frac{\sigma}{2\pi} + \mathcal{O}(u^{-1}), & \varphi &= \frac{\log(8u)}{2\pi} + \mathcal{O}(u^{-1}), \\ F &= \frac{1}{2\pi i} \log \frac{e^{i\sigma}}{8u} + \mathcal{O}(u^{-1}) \end{aligned} \quad (\text{B.8})$$

which, with the relation (3.14), reduces to (B.1) with an appropriate choice for  $\mu$ . Also, the value at  $u = 1$  is

$$\gamma(u = 1, \sigma) = \sin^2 \left( \frac{\pi}{2} \left\{ \frac{\sigma}{2\pi} \right\} \right) + \left\lfloor \frac{\sigma}{2\pi} \right\rfloor, \quad (\text{B.9})$$

where  $\{x\} \equiv x - \lfloor x \rfloor$  is the fractional part of  $x$  and  $\lfloor x \rfloor$  is the floor function. This is a smooth function with its second derivative being discontinuous at  $\sigma \in 2\pi\mathbb{Z}$ .

A natural question is whether we can obtain the 3D harmonic function (B.3) upon applying the extension formula (3.17). It turns out that that is not possible, because the expansion of  $F$  contains only  $Q_\nu$  and  $\mathcal{Q}_\nu$ , while the extension formula (3.17) only contains  $P_\nu$ . Below we study this in more detail.

## B.1 Partition of unity

One possible starting point is to ask the following question. Obviously

$$1 = \sqrt{u - \cos \sigma} \cdot \frac{1}{\sqrt{u - \cos \sigma}}. \quad (\text{B.10})$$

From the discussion around (3.5)–(3.7), we must be able to expand  $(u - \cos \sigma)^{-1/2}$  in terms of  $P_\nu(u)$  and  $Q_\nu(u)$ . What is the expansion?

By expanding  $(u - \cos \sigma)^{-1/2}$  in  $u^{-1}$  and collecting terms with the same power of  $e^{i\sigma}$ , it is straightforward to show

$$\frac{1}{\sqrt{u - \cos \sigma}} = \sum_{m=-\infty}^{\infty} e^{im\sigma} \frac{\Gamma(|m| + \frac{1}{2}) {}_2F_1(\frac{1}{4} + \frac{|m|}{2}, \frac{3}{4} + \frac{|m|}{2}; 1 + |m|; u^{-2})}{\Gamma(|m| + 1) \sqrt{\pi u} (2u)^{|m|}}. \quad (\text{B.11})$$

From the discussion around (3.5)–(3.7) and from the relations (A.7) and (A.8), the coefficient of  $e^{im\sigma}$  must be expressible as a linear combination of  $P_{|m|-1/2}(u)$  and  $Q_{|m|-1/2}(u)$ . We can determine the linear combination by looking at the behavior as  $u \rightarrow \infty$ . Because  ${}_2F_1(a, b; c; z) \rightarrow 1$  as  $z \rightarrow 0$ , the coefficient goes like  $u^{-|m|-1/2}$ . As  $u \rightarrow \infty$ , the behavior of  $P_{|m|-1/2}(u)$ ,  $Q_{|m|-1/2}(u)$  is

$$P_{|m|-1/2}(u) = \begin{cases} \mathcal{O}(u^{-1/2}, u^{-1/2} \log u) & (|m| = 0) \\ \mathcal{O}(u^{|m|-1/2}) & (|m| \geq 1) \end{cases}, \quad (\text{B.12})$$

$$Q_{|m|-1/2}(u) = \frac{\sqrt{\pi} \Gamma(|m| + 1/2)}{\Gamma(|m| + 1)} \frac{1}{(2u)^{|m|+1/2}} + \dots \quad (\text{B.13})$$

So, the coefficients in (B.11) must contain only  $Q_{|m|-1/2}(u)$  and no  $P_{|m|-1/2}(u)$ . After fixing the coefficients by comparison, we find that

$$\frac{1}{\sqrt{u - \cos \sigma}} = \frac{\sqrt{2}}{\pi} \sum_{m=-\infty}^{\infty} e^{im\sigma} Q_{|m|-1/2}(u). \quad (\text{B.14})$$

In other words,

$$1 = \sqrt{u - \cos \sigma} \cdot \frac{\sqrt{2}}{\pi} \left[ Q_{-1/2}(u) + \sum_{m=1}^{\infty} \left( e^{im\sigma} Q_{m-1/2}(u) + e^{-im\sigma} Q_{m-1/2}(u) \right) \right]. \quad (\text{B.15})$$

This is how we expand unity in terms of the basis of harmonic functions,  $P, Q$ .

## B.2 The supertube harmonic function expanded in $Q, \mathcal{Q}$

According to (3.12),

$$H = \frac{\sqrt{u - \cos \sigma}}{2\pi i} e^{\pm im\sigma} (\mathcal{Q}_{m-1/2} \pm i\sigma Q_{m-1/2}) \quad (\text{B.16})$$

is a harmonic function that has the monodromy

$$H \rightarrow H \pm \sqrt{u - \cos \sigma} e^{\pm im\sigma} Q_{m-1/2}. \quad (\text{B.17})$$

Combining this fact with the relation (B.15), we conclude that  $\gamma$ , which is harmonic and has the monodromy (B.7), must be given by

$$\begin{aligned} \gamma(u, \sigma) = & \frac{\sqrt{u - \cos \sigma}}{2\pi i} \frac{\sqrt{2}}{\pi} \left[ a(\mathcal{Q}_{-1/2} + i\sigma Q_{-1/2}) - b(\mathcal{Q}_{-1/2} - i\sigma Q_{-1/2}) \right. \\ & \left. + \sum_{m=1}^{\infty} \left( e^{im\sigma} (\mathcal{Q}_{m-1/2} + i\sigma Q_{m-1/2}) - e^{-im\sigma} (\mathcal{Q}_{m-1/2} - i\sigma Q_{m-1/2}) \right) \right] \end{aligned} \quad (\text{B.18})$$

with  $a + b = 1$ . The values of  $a, b$  cannot be determined only by monodromy. From (A.28b), the leading  $u \rightarrow \infty$  behavior of (B.18) is

$$\gamma \sim (a - b)(i\sigma - \log u). \quad (\text{B.19})$$

By comparing this with the desired behavior of  $\gamma$ , (B.8), we find that we must take  $a = b = 1/2$ . It is not difficult to check that, with this choice, (B.18) is indeed equal to (B.5).

On the other hand, using (A.19), the function  $\varphi$  in (B.4) can be written as

$$\begin{aligned} \varphi &= -\frac{1}{\sqrt{2}\pi^2} \sqrt{u - \cos \sigma} \mathcal{Q}_{-1/2} \\ &= -\frac{1}{2\sqrt{2}\pi^2} \sqrt{u - \cos \sigma} [(\mathcal{Q}_{-1/2} + i\sigma Q_{-1/2}) + (\mathcal{Q}_{-1/2} - i\sigma Q_{-1/2})]. \end{aligned} \quad (\text{B.20})$$

Combining this with (B.18), we finally find the expression for the 3D harmonic function  $F = \gamma + i\varphi$  in terms of  $Q, \mathcal{Q}$ :

$$\begin{aligned} F = & \frac{\sqrt{u - \cos \sigma}}{2\pi i} \frac{\sqrt{2}}{\pi} \left[ (\mathcal{Q}_{-1/2} + i\sigma Q_{-1/2}) \right. \\ & \left. + \sum_{m=1}^{\infty} \left( e^{im\sigma} (\mathcal{Q}_{m-1/2} + i\sigma Q_{m-1/2}) - e^{-im\sigma} (\mathcal{Q}_{m-1/2} - i\sigma Q_{m-1/2}) \right) \right]. \end{aligned} \quad (\text{B.21})$$

Some comments are in order. Using (A.28b), we see that the first line of (B.21) tends to the holomorphic term  $\log z$  in the 2D limit, which reproduces the desired 2D expression (B.1). Therefore, this line is required by matching. On the other hand, the two terms in the second line tend to  $z^m \log z$  and  $\bar{z}^m \log \bar{z}$ . These do not correspond to anything in the 2D harmonic

function  $f$ ; because they vanish in the 2D limit,  $u \rightarrow \infty$  ( $|z| \rightarrow 0$ ), their existence cannot be deduced from matching. The second term is even anti-holomorphic and guessing its existence from the holomorphic  $f(z)$  is far from obvious. However, when extending  $f$  to 3D, these terms are necessary for the monodromy  $\gamma \rightarrow \gamma + 1$  in the entire  $\mathbb{R}^3$ , as we saw above. Another interesting point is that, because  $Q_{m-1/2}(u)$  goes as  $\frac{1}{2} \log \frac{2}{u-1}$  as  $u \rightarrow 1$  (see (A.9b)), it seems that  $F$  is singular at  $u = 1$ . However, actually, the  $u \rightarrow 1$  limit is regular except at  $\sigma \in 2\pi\mathbb{Z}$  as can be seen from (B.9). Indeed, the sum of the leading contributions is

$$\sum_{m \in \mathbb{Z}} e^{im\sigma} Q_{m-1/2}(u) \sim \frac{1}{2} \log \frac{2}{u-1} \sum_{m \in \mathbb{Z}} e^{im\sigma} = \frac{1}{2} \log \frac{2}{u-1} \cdot 2\pi \sum_{k \in \mathbb{Z}} \delta(\sigma - 2\pi k). \quad (\text{B.22})$$

For  $\sigma \notin 2\pi\mathbb{Z}$ , this vanishes and leads to a regular  $u \rightarrow 1$  limit. For  $\sigma \in 2\pi\mathbb{Z}$ , we have a  $\delta$ -function singularity, but that is consistent with the fact that (B.9) is non-analytic at  $\sigma \in 2\pi\mathbb{Z}$ .

## C More examples

Here we present more examples of 2D harmonic functions to which we can apply the extension formula. In these examples, it turns out that the monodromy structure in 3D is different from that in 2D, which is puzzling. When we look for genuine microstates of black holes that involve codimension-2 sources, these examples should serve as useful data points.

### C.1 Constant- $\tau$ solutions with two stacks

In section 4.2.2, we studied 3D solutions based on the constant- $\tau$  solution in 2D with a single stack of  $N$  branes. Here, we consider 3D solutions based on the constant- $\tau$  solution in 2D with two stacks of  $N/2$  branes ( $N$  branes in total).

As the 2D solution, let us consider the situation where there are the two stacks (each of  $N/2$  branes) at  $z = 0, 1$ . The harmonic functions are

$$g = \frac{1}{(z(z-1))^{N/24}}, \quad f = \tau_0 g, \quad (\text{C.1})$$

where  $\tau_0$  is constant. The  $z^{-1}$  expansion of  $g$  is

$$g = \sum_{k=0}^{\infty} \frac{\Gamma(\frac{N}{24} + k)}{\Gamma(\frac{N}{24})} \frac{1}{k!} \frac{1}{z^{k + \frac{N}{12}}}. \quad (\text{C.2})$$

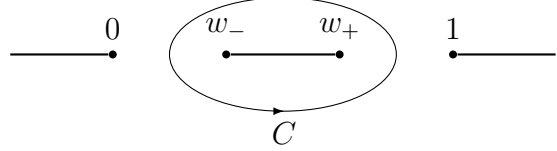
By a straightforward application of the extension formula (3.17), we find that the 3D harmonic function is

$$G = \frac{\Gamma(\frac{N}{12} + \frac{1}{2})^2}{\Gamma(\frac{N}{6})} \sqrt{\frac{u - \cos \sigma}{Z}} \frac{1}{2\pi i} \oint \frac{dt}{t-u} \left( \frac{t^2 - 1}{(t-u)Z} \right)^{\frac{N}{12} - \frac{1}{2}} {}_2F_1 \left( \frac{N}{24}, \frac{N}{12} + \frac{1}{2}; \frac{N}{12}; \frac{t^2 - 1}{4(t-u)Z} \right). \quad (\text{C.3})$$

If we go to the  $w$  coordinate using (3.25) with  $a = 4$ , this can be written as

$$G = \frac{\Gamma(\frac{N}{12} + \frac{1}{2})^2}{\Gamma(\frac{N}{6})} \sqrt{\frac{u - \cos \sigma}{Z}} \frac{1}{2\pi i} \oint_C \frac{(4w)^{\frac{N}{12} - \frac{1}{2}} dw}{\sqrt{w^2 - \frac{u}{Z}w + \frac{1}{4Z^2}}} {}_2F_1\left(\frac{N}{24}, \frac{N}{12} + \frac{1}{2}; \frac{N}{12}; w\right). \quad (\text{C.4})$$

The hypergeometric function  ${}_2F_1(\alpha, \beta; \gamma; z)$  has a branch cut along  $[1, \infty]$ . So, the cut structure and the contour  $C$  on the  $w$ -plane are as below:



$$\text{---} \bullet 0 \quad \bullet w_- \quad \bullet w_+ \quad \bullet 1 \text{---} \quad (\text{C.5})$$

The position of branes corresponds to the values of  $(u, \sigma)$  at which some cuts collide. We find that this can happen for  $w_+ = 1$  and  $w_- = 0$ , which gives the following brane positions:

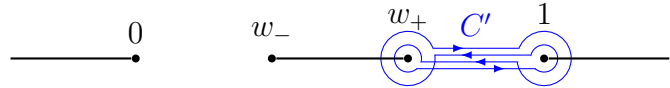
$$(u, \sigma) = (u_*, l), (\infty, \text{any}), \quad (\text{C.6})$$

where  $u_*$  was defined in (4.51).

In 2D, as we go around a stack of branes, the harmonic function gets multiplied by the phase  $e^{-\pi i N/12}$  as can be seen from (C.1). In 3D, what is the change in the contour when we go around the stack of branes at  $(u, \sigma) = (u_*, l)$ ? By carefully studying how the contour transforms, one finds that

$$C \rightarrow C + C' \quad (\text{C.7})$$

where  $C'$  is a Pochhammer contour:



$$\text{---} \bullet 0 \quad \bullet w_- \quad \bullet w_+ \quad \bullet 1 \text{---} \quad (\text{C.8})$$

In general, the contour integral along  $C + C'$  is not equal to  $e^{-\pi i N/12}$  times the contour integral along  $C$ . This is easiest to see in the  $u \rightarrow 1$  limit, in which  $w_+ = w_- = \frac{1}{2Z}$ . In this limit, the contour integral along  $C'$  diverges because it goes through the cut that collapses. This means that, if we approach the  $x_3$ -axis (where  $u = 1$ ) avoiding the branes,  $G$  is finite, but if go through the branes and approach the  $x_3$ -axis,  $G$  diverges. Therefore, the monodromy around branes of the 3D solution is different from that of the 2D solution. We do not have a good physical understanding of this puzzling result.

## C.2 Another non-constant $\tau$ solution with two stacks

As another example, let us look at the curve

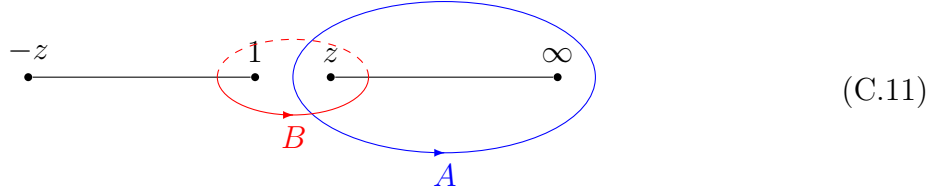
$$y^2 = (x^2 - \hat{z}^2)(x - 1). \quad (\text{C.9})$$

Either by looking at the discriminant or by finding the values of  $\hat{z}$  at which branch points collide, we see that this setup contains a stack of two branes at each of the points  $\hat{z} = -1, 0, 1$ ; namely, there are six branes in total. Unlike (4.39), there are no branes at  $\hat{z} = \infty$ . This curve can be obtained from (4.39) by a fractional linear transformation in  $\hat{z}$  to bring the brane at  $\hat{z} = \infty$  to finite  $\hat{z}$ .

We define the 2D harmonic functions as the period integrals of the torus (C.9),

$$\begin{aligned} g(z) &= \frac{1}{2} \int_A \frac{dx}{\sqrt{(x^2 - z^2)(x - 1)}} = \int_z^\infty \frac{dx}{\sqrt{(x^2 - z^2)(x - 1)}} = \frac{2\mathbf{K}\left(\frac{1+z}{1-z}\right)}{\sqrt{z-1}}, \\ f(z) &= \frac{1}{2} \int_B \frac{dx}{\sqrt{(x^2 - z^2)(x - 1)}} = i \int_1^z \frac{dx}{\sqrt{(z^2 - x^2)(x - 1)}} = \frac{\sqrt{2}i\mathbf{K}\left(\frac{z-1}{2z}\right)}{\sqrt{z}}. \end{aligned} \quad (\text{C.10})$$

The cuts and contours are taken as below:



We define  $\sqrt{(x^2 - z^2)(x - 1)}$  to be real and positive just below the cut  $[z, \infty]$ .

As we did for (4.45), we can find monodromy matrices as we go around branes in the  $\hat{z}$  space, by following how the cycles transform into each other. The result is:

$$M_{-1} = \begin{pmatrix} 1 & 2 \\ 0 & 1 \end{pmatrix}, \quad M_0 = \begin{pmatrix} -1 & 2 \\ -2 & 3 \end{pmatrix}, \quad M_1 = \begin{pmatrix} 1 & 0 \\ -2 & 1 \end{pmatrix}, \quad M_\infty = \begin{pmatrix} -1 & 0 \\ 0 & -1 \end{pmatrix}. \quad (\text{C.12})$$

These satisfy

$$M_1 M_0 M_{-1} = M_\infty. \quad (\text{C.13})$$

The monodromy matrix  $M_\infty = -\mathbf{1}$  is consistent with what we said below (4.12), because we are going around 6 branes; the solution there can be thought of as the limit of the current configuration in which all the branes collapse to a point. We can also consider going half around  $z = \infty$  counterclockwise as  $z \rightarrow e^{i\pi} z$ . The associated monodromy matrix is

$$M_\infty^{1/2} = \begin{pmatrix} 0 & 1 \\ -1 & 0 \end{pmatrix}. \quad (\text{C.14})$$

We can derive the 3D harmonic functions as follows. By setting  $x \rightarrow xz$  in (C.10) and expanding in  $z^{-1}$ , we find that

$$g(z) = \int_1^\infty \frac{dx}{\sqrt{(x^2 - 1)(zx - 1)}} = \sum_{k=0}^\infty \frac{\Gamma(\frac{1}{2} + k)}{\Gamma(\frac{1}{2})k!} \frac{1}{z^{k+\frac{1}{2}}} \int_1^\infty \frac{x^{-k-\frac{1}{2}} dx}{\sqrt{x^2 - 1}}. \quad (\text{C.15})$$

Using the dictionary to go from a 2D harmonic function (3.15) to the 3D one (3.17a), we find

$$\begin{aligned} G(u, \sigma) &= \sqrt{\frac{u - \cos \sigma}{Z}} \sum_{k=0}^{\infty} \int_1^{\infty} dx \frac{x^{-k-\frac{1}{2}} P_k(u)}{\sqrt{x^2 - 1} (2Z)^k} \\ &= \sqrt{\frac{u - \cos \sigma}{Z}} \int_1^{\infty} dx \sqrt{\frac{x}{(x^2 - 1)(x^2 - \frac{u}{Z}x + \frac{1}{4Z^2})}}, \end{aligned} \quad (\text{C.16})$$

where in the second equality we used the formula for the generating function of the Legendre polynomials,

$$\frac{1}{\sqrt{1 - 2tx + t^2}} = \sum_{k=0}^{\infty} P_k(x) t^k. \quad (\text{C.17})$$

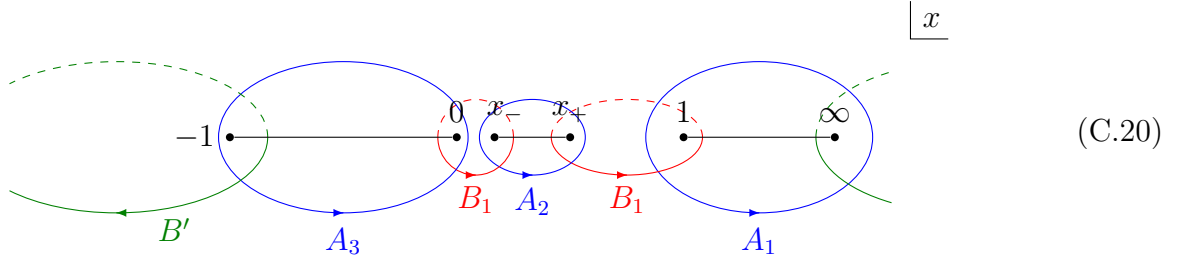
What is peculiar about the result (C.16) is the appearance of the genus-two Riemann surface,

$$y^2 = x(x^2 - 1) \left( x^2 - \frac{u}{Z}x + \frac{1}{4Z^2} \right). \quad (\text{C.18})$$

We can regard  $G$  in (C.16) as a period of this Riemann surface. The roots of the right-hand side of (C.18) are

$$x = 0, \quad \pm 1, \quad x_{\pm} \equiv \frac{1}{2Z} \left( u \pm \sqrt{u^2 - 1} \right). \quad (\text{C.19})$$

So, the branch cut structure of the genus-2 curve is as follows:



where we named various cycles. These cycles are not independent but satisfy

$$A_3 = -A_1 - A_2, \quad B' = B_1 + B_2. \quad (\text{C.21})$$

The contour used to define  $G$  in (C.16) is  $A_1$ , namely,

$$G = \oint_{A_1} \omega, \quad \omega = \frac{1}{2} \sqrt{\frac{u - \cos \sigma}{Z}} \frac{x}{y} dx. \quad (\text{C.22})$$

As we go from 2D to 3D, the cut on the left in (C.11) has split into two cuts.

To better understand the situation, we would like to study the monodromy as we go around branes. We can determine the location of branes by studying when the branch points collide. A short analysis tells us that the branes are at

$$(u, \sigma) = (u_*, l), (u_*, l - \pi), (\infty, \text{any}), \quad (\text{C.23})$$

where  $u_*$  was defined in (4.51) and we assumed that  $|Z| \geq 1/2$ . These correspond to the location of the branes in the 2D solution,  $\hat{z} = 1, -1, 0$ , respectively. By carefully following how the cycles transform into each other, we find the following monodromy matrices:

$$\begin{aligned} M_{-1} &= \begin{pmatrix} 1 & 2 & 2 & 0 \\ 0 & 1 & 0 & 0 \\ 0 & 0 & 1 & 0 \\ 0 & -2 & -2 & 1 \end{pmatrix}, & M_1 &= \begin{pmatrix} 1 & 0 & 0 & 0 \\ 0 & 1 & 0 & 0 \\ -2 & 0 & 1 & 0 \\ 0 & 0 & 0 & 1 \end{pmatrix}, \\ M_0 &= \begin{pmatrix} -1 & 0 & 2 & 0 \\ 0 & 1 & 0 & 0 \\ -2 & 0 & 3 & 0 \\ 0 & 2 & 0 & 1 \end{pmatrix}, & M_\infty &= \begin{pmatrix} -1 & -2 & 0 & 0 \\ 0 & 1 & 0 & 0 \\ 0 & 0 & -1 & 0 \\ 0 & 0 & -2 & 1 \end{pmatrix}. \end{aligned} \tag{C.24}$$

where we presented the matrices in the symplectic basis of  $(b_1, b_2, a_1, a_2)$ , where

$$a_1 = A_1, \quad b_1 = B_1, \quad a_2 = -A_3 = A_1 + A_2, \quad b_2 = B_2. \tag{C.25}$$

These matrices  $Sp(4, \mathbb{Z})$  are matrices satisfying

$$M^T J M = J, \quad J = \begin{pmatrix} 0 & \mathbf{1}_2 \\ -\mathbf{1}_2 & 0 \end{pmatrix}. \tag{C.26}$$

They also satisfy

$$M_1 M_0 M_{-1} = M_\infty. \tag{C.27}$$

We can also go halfway around all the branes counterclockwise, for which the monodromy matrix is

$$M_\infty^{1/2} = \begin{pmatrix} 0 & 1 & 1 & 0 \\ 0 & -1 & 0 & 0 \\ -1 & -1 & 0 & 0 \\ -1 & -1 & 1 & -1 \end{pmatrix}. \tag{C.28}$$

The 3D monodromy matrices (C.24), (C.28) correspond to the 2D monodromy matrices (C.12), (C.14). We can see that, if we take the submatrices of the 3D matrices by only keeping the  $(b_1, a_1)$  part, we recover the corresponding 2D matrices.

How should we define the other harmonic function  $F$ ? We want the 3D solution to have the same monodromy as the 2D solution. In 2D, for example, as we go around the  $\hat{z} = 1$  brane, cycle  $A$  turns into  $A - 2B$ , as can be read off from (C.12). In 3D, as we go around the  $(u_*, l)$  brane, the cycle  $A_1 = a_1$  goes to  $a_1 - 2b_1 = A_1 - 2B_1$ . So, this suggests that we define  $F$  by

$$F \stackrel{?}{=} \oint_{B_1} \omega. \tag{C.29}$$

What happens to this  $F$ , if we go around the  $(u_*, l - \pi)$  brane? In 2D, as we go around the  $\hat{z} = -1$  brane,  $B$  goes to  $B + 2A$  and thus  $f$  goes to  $f + 2g$ . However, in 3D, the monodromy matrix (C.24) says that the cycle  $B_1 = b_1$  goes to  $b_1 + 2b_2 + 2a_1 = B_1 + 2B_2 + 2A_1$ . This is not  $F + 2G$  but we have an extra contribution,  $2 \oint_{B_2} \omega$ . Therefore, the monodromy structure of the harmonic functions in 3D has changed from that in 2D! In other words, although we started in 2D with two harmonic functions  $(f, g)$  that transform under  $SL(2, \mathbb{Z})$ , we ended up in 3D with four harmonic functions that transform under  $Sp(4, \mathbb{Z})$ . Relatedly, the genus-one Riemann surface (torus) in 2D has become a genus-two Riemann surface. We do not have a good physical understanding of this puzzling situation.

## References

- [1] K. Behrndt, D. Lust and W. A. Sabra, “Stationary solutions of N=2 supergravity,” Nucl. Phys. B **510**, 264-288 (1998) doi:10.1016/S0550-3213(97)00633-0 [[arXiv:hep-th/9705169](#) [hep-th]].
- [2] J. P. Gauntlett, J. B. Gutowski, C. M. Hull, S. Pakis and H. S. Reall, “All supersymmetric solutions of minimal supergravity in five- dimensions,” Class. Quant. Grav. **20**, 4587 (2003) [[hep-th/0209114](#)].
- [3] B. Bates and F. Denef, “Exact solutions for supersymmetric stationary black hole composites,” JHEP **1111**, 127 (2011) [[hep-th/0304094](#)].
- [4] I. Bena and N. P. Warner, “One ring to rule them all ... and in the darkness bind them?,” Adv. Theor. Math. Phys. **9**, 667 (2005) [[hep-th/0408106](#)].
- [5] J. P. Gauntlett and J. B. Gutowski, “General concentric black rings,” Phys. Rev. D **71**, 045002 (2005) [[hep-th/0408122](#)].
- [6] I. Bena and N. P. Warner, “Bubbling supertubes and foaming black holes,” Phys. Rev. D **74**, 066001 (2006) [[hep-th/0505166](#)].
- [7] P. Berglund, E. G. Gimon and T. S. Levi, “Supergravity microstates for BPS black holes and black rings,” JHEP **0606**, 007 (2006) [[hep-th/0505167](#)].
- [8] P. Meessen and T. Ortin, “The Supersymmetric configurations of N=2, D=4 supergravity coupled to vector supermultiplets,” Nucl. Phys. B **749**, 291-324 (2006) doi:10.1016/j.nuclphysb.2006.05.025 [[arXiv:hep-th/0603099](#) [hep-th]].
- [9] I. Bena, S. Giusto, R. Russo, M. Shigemori and N. P. Warner, “Habemus Superstratum! A constructive proof of the existence of superstrata,” JHEP **05**, 110 (2015) doi:10.1007/JHEP05(2015)110 [[arXiv:1503.01463](#) [hep-th]].

- [10] M. Shigemori, “Superstrata,” *Gen. Rel. Grav.* **52**, no.5, 51 (2020) doi:10.1007/s10714-020-02698-8 [[arXiv:2002.01592](#) [hep-th]].
- [11] J. de Boer, S. El-Showk, I. Messamah and D. Van den Bleeken, “A Bound on the entropy of supergravity?,” *JHEP* **1002**, 062 (2010) [[arXiv:0906.0011](#) [hep-th]].
- [12] M. Shigemori, “Counting Superstrata,” *JHEP* **10**, 017 (2019) doi:10.1007/JHEP10(2019)017 [[arXiv:1907.03878](#) [hep-th]].
- [13] D. R. Mayerson and M. Shigemori, “Counting D1-D5-P microstates in supergravity,” *SciPost Phys.* **10**, no.1, 018 (2021) doi:10.21468/SciPostPhys.10.1.018 [[arXiv:2010.04172](#) [hep-th]].
- [14] I. Bena, S. D. Hampton, A. Houppe, Y. Li and D. Toulukas, “The (amazing) super-maze,” *JHEP* **03**, 237 (2023) doi:10.1007/JHEP03(2023)237 [[arXiv:2211.14326](#) [hep-th]].
- [15] I. Bena, N. Čeplak, S. D. Hampton, A. Houppe, D. Toulukas and N. P. Warner, “Themelia: the irreducible microstructure of black holes,” [[arXiv:2212.06158](#) [hep-th]].
- [16] I. Bena, A. Houppe, D. Toulukas and N. P. Warner, “Maze Topiary in Supergravity,” [[arXiv:2312.02286](#) [hep-th]].
- [17] B. Eckardt and Y. Li, “The 1/4-BPS building blocks of brane interactions,” [[arXiv:2312.13269](#) [hep-th]].
- [18] I. Bena and R. Dulac, “Born-Infeld Supermaze Waves,” [[arXiv:2312.13447](#) [hep-th]].
- [19] M. Park and M. Shigemori, “Codimension-2 solutions in five-dimensional supergravity,” *JHEP* **1510**, 011 (2015) doi:10.1007/JHEP10(2015)011 [[arXiv:1505.05169](#) [hep-th]].
- [20] J. J. Fernandez-Melgarejo, M. Park and M. Shigemori, “Non-Abelian Supertubes,” *JHEP* **12**, 103 (2017) doi:10.1007/JHEP12(2017)103 [[arXiv:1709.02388](#) [hep-th]].
- [21] M. Shigemori, “Interpolating between multi-center microstate geometries,” *JHEP* **09**, 010 (2021) doi:10.1007/JHEP09(2021)010 [[arXiv:2105.11639](#) [hep-th]].
- [22] D. Mateos and P. K. Townsend, “Supertubes,” *Phys. Rev. Lett.* **87**, 011602 (2001) [[hep-th/0103030](#)].
- [23] R. Emparan, D. Mateos and P. K. Townsend, “Supergravity supertubes,” *JHEP* **07**, 011 (2001) doi:10.1088/1126-6708/2001/07/011 [[arXiv:hep-th/0106012](#) [hep-th]].
- [24] N. A. Obers and B. Pioline, “U duality and M theory,” *Phys. Rept.* **318**, 113-225 (1999) doi:10.1016/S0370-1573(99)00004-6 [[arXiv:hep-th/9809039](#) [hep-th]].

- [25] J. de Boer and M. Shigemori, “Exotic Branes in String Theory,” *Phys. Rept.* **532**, 65-118 (2013) doi:10.1016/j.physrep.2013.07.003 [[arXiv:1209.6056](#) [hep-th]].
- [26] E. Bergshoeff, R. Kallosh and T. Ortin, “Stationary axion / dilaton solutions and supersymmetry,” *Nucl. Phys. B* **478**, 156-180 (1996) doi:10.1016/0550-3213(96)00408-7 [[arXiv:hep-th/9605059](#) [hep-th]].
- [27] J. B. Gutowski and H. S. Reall, “General supersymmetric AdS(5) black holes,” *JHEP* **04**, 048 (2004) doi:10.1088/1126-6708/2004/04/048 [[arXiv:hep-th/0401129](#) [hep-th]].
- [28] J. B. Gutowski and W. Sabra, “General supersymmetric solutions of five-dimensional supergravity,” *JHEP* **10**, 039 (2005) doi:10.1088/1126-6708/2005/10/039 [[arXiv:hep-th/0505185](#) [hep-th]].
- [29] G. Dall’Agata, S. Giusto and C. Ruef, “U-duality and non-BPS solutions,” *JHEP* **02**, 074 (2011) doi:10.1007/JHEP02(2011)074 [[arXiv:1012.4803](#) [hep-th]].
- [30] F. Denef, “Supergravity flows and D-brane stability,” *JHEP* **08**, 050 (2000) doi:10.1088/1126-6708/2000/08/050 [[arXiv:hep-th/0005049](#) [hep-th]].
- [31] I. Bena, J. de Boer, M. Shigemori and N. P. Warner, “Double, Double Supertube Bubble,” *JHEP* **10**, 116 (2011) doi:10.1007/JHEP10(2011)116 [[arXiv:1107.2650](#) [hep-th]].
- [32] Problem 5.1 in J. D. Jackson, “Classical Electrodynamics,” Wiley, 1998, ISBN 978-0-471-30932-1.
- [33] N. B. Backhouse, “The Resonant Legendre Equation,” *J. Math. Anal. Appl.* **117**, 310 (1986).
- [34] N. Seiberg and E. Witten, “Electric - magnetic duality, monopole condensation, and confinement in N=2 supersymmetric Yang-Mills theory,” *Nucl. Phys. B* **426**, 19 (1994) Erratum: [*Nucl. Phys. B* **430**, 485 (1994)] doi:10.1016/0550-3213(94)90124-4, 10.1016/0550-3213(94)00449-8 [[hep-th/9407087](#)].
- [35] N. Seiberg and E. Witten, “Monopoles, duality and chiral symmetry breaking in N=2 supersymmetric QCD,” *Nucl. Phys. B* **431**, 484-550 (1994) doi:10.1016/0550-3213(94)90214-3 [[arXiv:hep-th/9408099](#) [hep-th]].
- [36] B. R. Greene, A. D. Shapere, C. Vafa and S. T. Yau, “Stringy Cosmic Strings and Noncompact Calabi-Yau Manifolds,” *Nucl. Phys. B* **337**, 1 (1990). doi:10.1016/0550-3213(90)90248-C
- [37] C. Vafa, “Evidence for F theory,” *Nucl. Phys. B* **469**, 403-418 (1996) doi:10.1016/0550-3213(96)00172-1 [[arXiv:hep-th/9602022](#) [hep-th]].

- [38] A. Sen, “F theory and orientifolds,” Nucl. Phys. B **475**, 562-578 (1996) doi:10.1016/0550-3213(96)00347-1 [[arXiv:hep-th/9605150](#) [hep-th]].
- [39] K. Dasgupta and S. Mukhi, “F theory at constant coupling,” Phys. Lett. B **385**, 125-131 (1996) doi:10.1016/0370-2693(96)00875-1 [[arXiv:hep-th/9606044](#) [hep-th]].
- [40] I. Bena and N. P. Warner, “Resolving the Structure of Black Holes: Philosophizing with a Hammer,” [[arXiv:1311.4538](#) [hep-th]].
- [41] A. Sen, “Arithmetic of Quantum Entropy Function,” JHEP **08**, 068 (2009) doi:10.1088/1126-6708/2009/08/068 [[arXiv:0903.1477](#) [hep-th]].  
 ”status”: 404, ”message”: ”PID does not exist.”
- [42] A. Dabholkar, J. Gomes, S. Murthy and A. Sen, “Supersymmetric Index from Black Hole Entropy,” JHEP **04**, 034 (2011) doi:10.1007/JHEP04(2011)034 [[arXiv:1009.3226](#) [hep-th]].
- [43] A. Chowdhury, R. S. Garavuso, S. Mondal and A. Sen, “Do All BPS Black Hole Microstates Carry Zero Angular Momentum?,” JHEP **04**, 082 (2016) doi:10.1007/JHEP04(2016)082 [[arXiv:1511.06978](#) [hep-th]].
- [44] A. S. Schwarz, “FIELD THEORIES WITH NO LOCAL CONSERVATION OF THE ELECTRIC CHARGE,” Nucl. Phys. B **208** (1982), 141-158 doi:10.1016/0550-3213(82)90190-0
- [45] M. G. Alford, K. Benson, S. R. Coleman, J. March-Russell and F. Wilczek, “The Interactions and Excitations of Nonabelian Vortices,” Phys. Rev. Lett. **64** (1990), 1632 [erratum: Phys. Rev. Lett. **65** (1990), 668] doi:10.1103/PhysRevLett.64.1632
- [46] J. Preskill and L. M. Krauss, “Local Discrete Symmetry and Quantum Mechanical Hair,” Nucl. Phys. B **341** (1990), 50-100 doi:10.1016/0550-3213(90)90262-C
- [47] J. A. Harvey and A. B. Royston, “Localized modes at a D-brane-O-plane intersection and heterotic Alice atrings,” JHEP **04**, 018 (2008) doi:10.1088/1126-6708/2008/04/018 [[arXiv:0709.1482](#) [hep-th]].
- [48] T. Okada and Y. Sakatani, “Defect branes as Alice strings,” JHEP **03**, 131 (2015) doi:10.1007/JHEP03(2015)131 [[arXiv:1411.1043](#) [hep-th]].